Titanium Hydrazides Supported by Diamide-Amine and Related Ligands: A Combined Experimental and DFT Study

Jonathan D. Selby,[†] Catherine D. Manley,[†] Andrew D. Schwarz,[†] Eric Clot,*[,‡] and Philip Mountford*[,†]

Chemistry Research Laboratory, University of Oxford, Mansfield Road, Oxford OX1 3TA, U.K., and Institut Charles Gerhardt Montpellier, UMR 5253 CNRS-UM2-UM1-ENSCM, cc 1501, Place Eugène Bataillon, 34095 Montpellier Cedex 5, France

Received August 25, 2008

This paper reports a general method for the synthesis of new terminal titanium diphenyl hydrazido(2−) complexes containing dianionic N_3- and N_4-donor ligands, along with new hydrazido synthons. Reaction of $Ti(N^tBu)Cl_2(py)_3$ or $Ti(N^tBu)Cl_2(py')_3$ (py′ = 4-$NC_5H_4{}^tBu$) with Ph_2NNH_2 gave excellent yields of the corresponding monomeric hydrazides $Ti(NNPh_2)Cl_2(L)_3$ (L = py (**7**) or py′), which have been structurally characterized. Application of a dynamic vacuum to **7** formed $[Ti(NNPh_2)Cl_2(py)_2]_2$ (**4**). Both **4** and **7** are entry points to new titanium hydradizo complexes on reaction with metalated reagents. In this way, four new five-coordinate diamide-amine complexes $Ti(NNPh_2)$("N_2N")(py) were made ("N_2N" = $MeN(CH_2CH_2NSiMe_3)_2$, $Me_3SiN(CH_2CH_2NSiMe_3)_2$, $MeN(CH_2CH_2CH_2NSiMe_3)_2$, (2-$NC_5H_4$)C(Me)$(CH_2NSiMe_3)_2$) and structurally characterized. Five- and six-coordinate terminal titanium hydrazides containing dianionic N_4- or O_2N_2-donor ligands were also synthesized from **4** by an analogous method. The identity of the "N_2N" ligand affects the Ti═N_α and N_α−N_β distances of the Ti═N−NPh_2 functional group. A detailed DFT analysis of the bonding in these and a range of model complexes is presented using molecular orbital and natural bond orbital methods. The competition between N(amide) and N(hydrazide) Ti($3d_\pi$)−N($2p_\pi$) interactions has an indirect and significant effect on the N_α−N_β bond.

Introduction

Group 4 imido complexes (L)M═NR (R is usually alkyl or aryl, L is a supporting ligand (set)) have been a focus of ongoing activity for nearly 20 years.[1−6] As well as being of interest from the point of view of fundamental bonding and reactivity (typically focusing on the M═NR bond), practical applications have been found in the catalytic hydroamination of C−C multiple bonds, olefin polymerization, and metal organic chemical vapor deposition. In contrast, the corresponding chemistry of terminal hydrazide complexes (L)M═NNR_2 (R is alkyl or aryl) has barely been explored for these early metals. As summarized below, group 4 hydrazide chemistry has nonetheless already established the potential for exciting and significant departures from the norms expected from the imido analogues. However, there are currently no guiding principles for selecting the most appropriate supporting ligand sets to maximize the potential of this chemistry. This paper reports the synthesis and electronic structures of a new class of titanium hydrazide complex for advancing the chemistry of the Ti═NNR_2 functional group.

From a more general perspective, the chemistry of metal-bound NNR_2 species is of considerable interest in the context of the biological and synthetic fixation and activation of dinitrogen.[7−15] Chatt, Pickett, and co-workers showed experimentally that the conversion of N_2 to NH_3 starting from highly reducing zerovalent group 6 tetraphosphine complexes proceeds via (L)M−NNH_2 species.[16−19] Using a tris(amide)-amine ligand platform, Schrock et al. demonstrated the catalytic conversion of N_2 to NH_3, again via a Mo−NNH_2 intermediate, employing sequential reduction and protonation steps.[10,20] Tuczek has reported detailed DFT studies of both the Chatt[21] and Schrock[22] catalytic cycles, confirming the importance of M−NNH_2 species and the reduction-assisted N_α−N_β bond cleavage. The stoichiometric reactions of group 6 M−NNH_2 species with organic substrates have also been comprehensively studied. Reactions typically take place at the terminal β-NH_2 group, via condensation reactions or insertion into N−H.[13−15] Subsequent reductive N_α−N_β bond cleavage can yield organic fragments such as

* Corresponding authors. E-mail: philip.mountford@chem.ox.ac.uk; clot@univ-montp2.fr.
[†] University of Oxford.
[‡] Institut Charles Gerhardt Montpellier.

(1) Wigley, D. E. *Prog. Inorg. Chem.* **1994**, *42*, 239.
(2) Duncan, A. P.; Bergman, R. G. *Chem. Rec.* **2002**, *2*, 431.
(3) Odom, A. L. *Dalton Trans.* **2005**, 225.
(4) Hazari, N.; Mountford, P. *Acc. Chem. Res.* **2005**, *38*, 839.
(5) Bolton, P. D.; Mountford, P. *Adv. Synth. Catal.* **2005**, *347*, 355.
(6) Fout, A. R.; Kilgore, U. J.; Mindiola, D. J. *Chem.−Eur. J.* **2007**, *13*, 9428.
(7) Fryzuk, M. D. *Chem. Rec.* **2003**, *3*, 2.
(8) Kozak, C. M.; Mountford, P. *Angew. Chem., Int. Ed.* **2004**, *43*, 1186.
(9) MacKay, B. A.; Fryzuk, M. D. *Chem. Rev.* **2004**, *104*, 385.
(10) Schrock, R. R. *Acc. Chem. Res.* **2005**, *38*, 955.
(11) Chirik, P. J. *Dalton Trans.* **2007**, 16.
(12) Ohki, Y.; Fryzuk, M. D. *Angew. Chem., Int. Ed.* **2007**, *46*, 3180.
(13) Fryzuk, M. D.; Johnson, S. A. *Coord. Chem. Rev.* **2000**, *200−202*, 379.
(14) Hidai, M. *Chem. Rev.* **1995**, *95*, 1115.
(15) Hidai, M. *Coord. Chem. Rev.* **1999**, *185−186*, 99.
(16) Chatt, J.; Pearman, A. J.; Richards, R. L. *Nature* **1975**, *253*, 39.
(17) Pickett, C. J.; Leigh, G. J. *J. Chem. Soc., Chem. Commun.* **1981**, 1033.
(18) Hussain, W.; Leigh, G. J.; Pickett, C. J. *J. Chem. Soc., Chem. Commun.* **1982**, 747.
(19) Pickett, C. J.; Talamarin, J. *Nature* **1985**, *317*, 652.
(20) Yandulov, D. V.; Schrock, R. R. *Science* **2003**, 76.
(21) Stephan, G. C.; Sivasankar, C.; Studt, F.; Tuczek, F. *Chem.−Eur. J.* **2008**, *14*, 644.
(22) Studt, F.; Tuczek, F. *Angew. Chem., Int. Ed.* **2005**, *44*, 5639.

10.1021/om8007597 CCC: $40.75
Publication on Web 11/14/2008

pyrroles and pyridines. Notably, direct reaction of the $M-N_\alpha$ bond with unsaturated substrates is not seen. Furthermore, structural,[23,24] spectroscopic,[25] and DFT computational[21,22,26,27] data all suggest that the NNR_2 ligand in these group 6 complexes is best viewed as a neutral *isodiazene* ligand ($:N{=}NR_2$) rather than a hydrazide(2−) species $[N-NR_2]^{2-}$.

The first reported terminal titanium hydrazide was $Cp_2Ti\{NN(SiMe_3)_2\}$, prepared from Cp_2TiCl_2 and the thermally sensitive $N_2(SiMe_3)_2$ (dec > −35 °C).[28] There have been no reactivity or structural reports for this system, and the inconvenient nature of $N_2(SiMe_3)_2$ may have limited its development. Bergman reported and structurally characterized the first zirconium hydrazide, namely, $Cp_2Zr(NNPh_2)(DMAP)$,[29] and Odom was the first to report a structurally authenticated titanium hydrazide.[30] Since this report in 2004, only a handful of other terminal group 4 hydrazides have been structurally characterized.[31−35] As part of this early work, we reported structural and DFT studies of homologous Ti=NR (imido) and $Ti{=}NNPh_2$ systems, the first study of this type for group 4. These showed that for the early transition metals, $NNPh_2$ is best viewed as a hydrazide(2−) ligand analogous to imide(2−), rather than an isodiazene moiety.[31] One could expect early and later metal−NNR_2 systems (i.e., hydrazide and isodiazene) to differ in much the same way as Schrock alkylidenes and Fischer carbenes.[36]

Because of its apparent relationship to the corresponding Ti=NR systems, one of the main interests in the group 4 $M{=}NNR_2$ functional group concerns its reactivity with unsaturated organic substrates.[37] Bergman's transient $Cp_2Zr(NNPh_2)$ system underwent $N_\alpha-N_\beta$ bond cleavage reactions with alkynes and CO. Surprisingly, $Zr{=}NNR_2$/RCCR cycloaddition products (well known[2] for the corresponding imido systems $Cp_2Zr(NR)$) were not observed. Subsequent work from our own group used the macrocycle-supported complexes $Ti(NNPh_2)(Me_4taa)$ (H_2Me_4taa = tetramethyldibenzotetraaza[14]annulene[38]). On reaction with TolNCO or CO_2, these gave the first well-defined $M{=}N_\alpha$ [2+2] cycloaddition reactions of any group 4 $M{=}NNR_2$ functional group.[39] Woo et al. reported hydrazide ligand transfer reactions for the corresponding $Ti(NNR_2)(TTP)$ (H_2TTP = tetra-*p*-tolylporphyrin) system with *p*-chlorobenzaldehyde, which gave the corresponding hydrazones, also with the $N_\alpha-N_\beta$ bond remaining intact.[40] In contrast, Gade and co-workers once again encountered hydrazide $N_\alpha-N_\beta$ bond cleavage reactions on reaction of the diamide-amine-supported $Zr(N_2N^{py*})(NNPh_2)(py)$ (**1**, eq 1) with ^{t}BuNC, Ph_3PSe, or propylene sulfide (N_2N^{py*} = (2-NC_5H_4)C(Me)($CH_2NSiMe_2{}^tBu)_2$).[35]

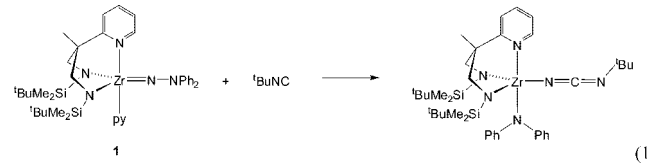

1 (1)

In addition to the above stoichiometric reactions of isolated complexes, terminal titanium hydrazides have been implicated (but not directly observed) in the catalytic hydrohydrazination[30,41−47] and iminohydrazination[32,46] of alkynes and in the synthesis of indoles[3,43,45] and tryptamines.[44] In these reactions, typically leading to a hydrazone or its equivalent, a [2+2] cycloaddition reaction between $Ti{=}NNR_2$ and an alkyne (or allene) is considered to be the key N−C bond forming step. Little, if anything, is directly known about these processes or the intermediates involved.

We recently reported[34] that reaction of the diamide-amine-supported complex $Ti(N_2N^{C_2,Me})(NNPh_2)(py)$ (**2**, *vide infra*) with PhCCMe did not give the expected [2+2] cycloaddition product, and once again a $N_\alpha-N_\beta$ bond cleavage product, $Ti(N_2N^{C_2,Me})\{NC(Ph)C(Me)NPh_2\}(py)$ (**3**), was formed (eq 2). In addition, reaction of **3** with Ph_2NNH_2 regenerated **2** to form the *cis*-1,2-diamino alkene $PhC(NH_2)C(Me)NPh_2$. This is a unique and unprecedented transformation of alkynes, which was also found to be catalytic in either **2** or **3**.

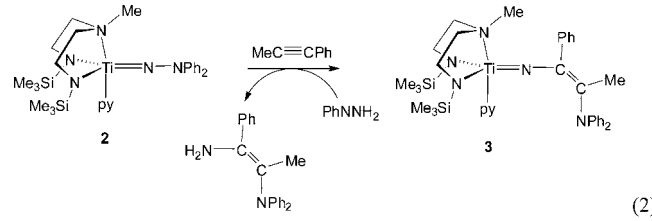

(2)

The rate and selectivity of the new transformation in eq 2 (and Bergman and Gade's earlier, noncatalytic analogues) should undoubtedly depend on the nature of the strongly π-donating diamide-donor (or related) ligand set. Indeed such chelating anionic nitrogen ligands have been very fruitful for developing the chemistry of early transition metal−ligand multiple bond chemistry during the last 10−15 years.[38,48−54] We note in particular Schrock's tris(amide)-amine ("tren") systems, which were crucial in that group's discovery of the synthetic catalytic conversion of N_2 to NH_3.[10,49] Polyamide-based ligands have also been important in the growing field of group 4 N_2 activation chemistry.[12] Therefore, as a platform for future developments in this field, we report in detail here the synthesis and molecular and electronic structures of a range of new titanium hydrazide complexes with N_3-, N_4-diamide-donor (and related) ligands, along with new entry synthons for titanium hydrazide chemistry. Part of this work has been communicated.[34]

Results and Discussion

Ligand Choices. Chart 1 illustrates the ligands used in this study. These chelating, dianionic ligands should provide well-defined, relatively nonlabile environments for studying compounds of the type $(L)Ti{=}NNR_2$, and the hard N- and O-donors are compatible with the desired Ti(+4) oxidation state. They have been widely used in early transition metal chemistry and metal−ligand multiple bond chemistry[4,23,24,38,39,50,51,55−65] and

(23) Allen, F. H.; Kennard, O. *Chem. Des. Automation News* **1993**, *8*, 1. and 31.
(24) Fletcher, D. A.; McMeeking, R. F.; Parkin, D. *J. Chem. Inf. Comput. Sci.* **1996**, *36*, 746 (The United Kingdom Chemical Database Service).
(25) Lehnert, N.; Tuczek, F. *Inorg. Chem.* **1999**, *38*, 1659.
(26) Mersmann, K.; Horn, K. H.; Bores, N.; Lehnert, N.; Studt, F.; Paulat, F.; Peters, G.; Ivanovic-Burmazovic, I.; van Eldik, R.; Tuczek, F. *Inorg. Chem.* **2005**, *44*, 3031.
(27) Lehnert, N.; Tuczek, F. *Inorg. Chem.* **1999**, *38*, 1671.
(28) Wiberg, N.; Haring, H.-W.; Huttner, G.; Friedrich, P. *Chem. Ber.* **1978**, *111*, 2708.
(29) Walsh, P. J.; Carney, M. J.; Bergman, R. G. *J. Am. Chem. Soc.* **1991**, *113*, 6343.
(30) Li, Y.; Shi, Y.; Odom, A. L. *J. Am. Chem. Soc.* **2004**, *126*, 1794.
(31) Parsons, T. B.; Hazari, N.; Cowley, A. R.; Green, J. C.; Mountford, P. *Inorg. Chem.* **2005**, *44*, 8442.
(32) Banerjee, S.; Odom, A. L. *Organometallics* **2006**, *25*, 3099.
(33) Patel, S.; Li, Y.; Odom, A. L. *Inorg. Chem.* **2007**, *46*, 6373.
(34) Selby, J. D.; Manley, C. D.; Felix, M.; Schwarz, A. D.; Clot, E.; Mountford, P. *Chem. Commun.* **2007**, 4937.
(35) Herrmann, H.; Fillol, J. L.; Wadepohl, H.; Gade, L. H. *Angew. Chem., Int. Ed.* **2007**, *46*, 8426.
(36) Crabtree, R. H. *The Organometallic Chemistry of the Transition Metals*, 4th ed.; WileyBlackwell: London, 2005.
(37) Mindiola, D. J. *Angew. Chem., Int. Ed.* **2008**, *47*, 1557.

Chart 1. The Ligands Used in This Contribution and Their Abbreviations (Formal Anionic Charges Omitted for Clarity)

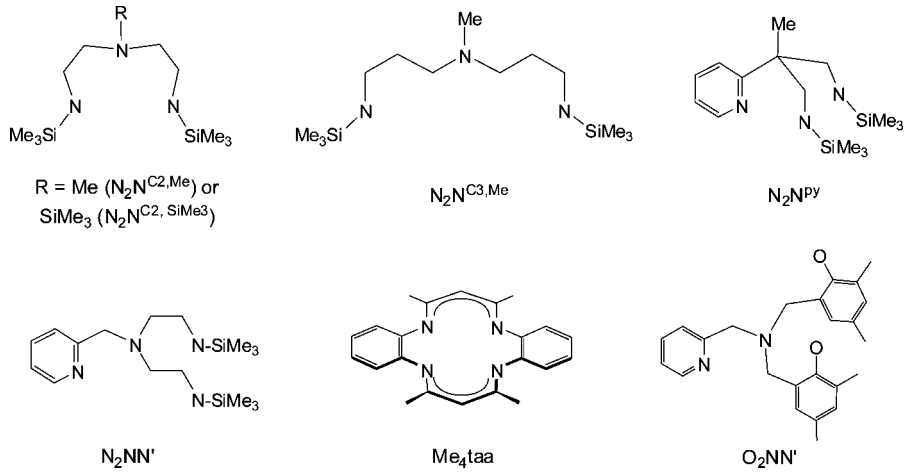

allow variation of the metal's coordination number and steric accessibility. They differ in bite angle, hemilability (or otherwise), and π-donor ability.

Development of a Synthetic Strategy to New Families of Hydrazide Complexes. While hydrazide complexes (L)Ti=NNR$_2$ are rather limited in number, several different synthetic strategies have been used for their preparation. Wiberg[28] and Woo[40] employed Me$_3$SiCl or LiCl elimination protocols, respectively, starting from the corresponding dichloride precusors (L)TiCl$_2$ (L = Cp$_2$ or TTP). We showed that Ti(Me$_4$taa)(N^{t}Bu) reacted with Ph$_2$NNH$_2$ to form Ti(Me$_4$taa)(NNPh$_2$) and ^{t}BuNH$_2$ via a protonolysis type reaction[39] reminiscent of the well-established *tert*-butyl imide/aniline exchange protocols used to form aryl imides.[4,6,66−68] Protonolysis reactions of bis(dimethylamido) compounds (L)Ti(NMe$_2$)$_2$ with several different hydrazines RR′NNH$_2$ (R = R = alkyl or aryl; R = aryl, R′ = H) have also afforded both terminal and bridging hydrazido derivatives.[30,33]

Although protonolysis procedures appeared attractive for preparing the target diamide-amine hydrazide complexes (avoiding potentially reducing anionic reagents), they were unsatisfactory due to concomitant protonolysis side-reactions of the supporting ligands. For example, reaction of Ti($N_2N^{C_2,SiMe_3}$)(N^{t}Bu)(py)[69] with Ph$_2$NNH$_2$ in C$_6$D$_6$ gave less than ca. 35% conversion to the target Ti($N_2N^{C_2,SiMe_3}$)(NNPh$_2$)(py) (*vide infra*). The remainder of the Ti($N_2N^{C_2,SiMe_3}$)(N^{t}Bu)(py) was consumed to form the protio ligand H$_2N_2N^{C_2,SiMe_3}$ and unknown species. Analogous results were found for certain other *tert*-butyl imido titanium complexes of the target ligands. Gade and co-workers have encountered similar difficulties starting from Ti(N_2N^{py})(NMe$_2$)$_2$.[70] The amido nitrogens of N$_3$- and N$_4$-donor supporting ligands of the type $N_2N^{C_n,R}$, N_2N^{py}, and N_2NN' are therefore prone to protonolysis reactions at a rate competitive with those of the target Ti=N^{t}Bu or Ti−NMe$_2$ leaving groups. This is in contrast to the Ti(Me$_4$taa)(N^{t}Bu) system, which underwent imide protonolysis with Ph$_2$NNH$_2$ without loss of H$_2$Me$_4$taa.[39,59] The difference may be partially attributable to the charge delocalization within the Me$_4$taa backbone, making the formally anionic ligands less Brønsted basic. Odom's successful conversion of Ti(dmpa)(NMe$_2$)$_2$ to Ti(dmpa)(NNMe$_2$)(^{t}Bubipy) might be explained in a similar way (dmpa = *N,N*-di(pyrrolyl-R-methyl)-*N*-methylamine; ^{t}Bubipy = di-*tert*-butylbipyridine).[30]

(38) Mountford, P. *Chem. Soc. Rev.* **1998**, *27*, 105.
(39) Blake, A. J.; McInnes, J. M.; Mountford, P.; Nikonov, G. I.; Swallow, D.; Watkin, D. J. *J. Chem. Soc., Dalton Trans.* **1999**, 379.
(40) Thorman, J. L.; Woo, L. K. *Inorg. Chem.* **2000**, *39*, 1301.
(41) Johnson, J. S.; Bergman, R. G. *J. Am. Chem. Soc.* **2001**, *123*, 2923.
(42) Cao, C.; Shi, Y.; Odom, A. L. *Org. Lett.* **2002**, *4*, 2853.
(43) Ackermann, L.; Born, R. *Tetrahedron Lett.* **2004**, *45*, 9541.
(44) Khedkar, V.; Tillack, A.; Michalik, M.; Beller, M. *Tetrahedron Lett.* **2004**, *45*, 3123.
(45) Tillack, A.; Jiao, H.; Garcia Castro, I.; Hartung, C. G.; Beller, M. *Chem.−Eur. J.* **2004**, *10*, 2410.
(46) Banerjee, S.; Shi, Y.; Cao, C.; Odom, A. L. *J. Organomet. Chem.* **2005**, *690*, 5066.
(47) Banerjee, S.; Barnea, E.; Odom, A. L. *Organometallics* **2008**, *27*, 1005.
(48) Brand, H.; Arnold, J. *Coord. Chem. Rev.* **1995**, *140*, 137.
(49) Schrock, R. R. *Acc. Chem. Res.* **1997**, *30*, 9.
(50) Gade, L. H. *Chem. Commun.* **2000**, 173.
(51) Gade, L. H.; Mountford, P. *Coord. Chem. Rev.* **2001**, *216−217*, 65.
(52) Bourget-Merle, L.; Lappert, M. F.; Severn, J. R. *Chem. Rev.* **2002**, *102*, 3031.
(53) Bigmore, H. R.; Lawrence, S. C.; Mountford, P.; Tredget, C. S. *Dalton Trans.* **2005**, 635.
(54) Kempe, R. *Angew. Chem., Int. Ed. Engl.* **2000**, *39*, 468.
(55) Lowes, T. A.; Ward, B. D.; Whannel, R. A.; Dubberley, S. R.; Mountford, P. *Chem. Commun.* **2005**, 113.
(56) Mountford, P.; Swallow, D. *J. Chem. Soc., Chem. Commun.* **1995**, 2357.
(57) Blake, A. J.; Mountford, P.; Nikonov, G. I.; Swallow, D. *Chem. Commun.* **1996**, 1835.
(58) Swallow, D.; Dunn, S. C.; Nikonov, G. I.; Mountford, P. *Abstr. Papers Am. Chem. Soc.* **1996**, *211*, 78.
(59) Swallow, D.; McInnes, J. M.; Mountford, P. *J. Chem. Soc., Dalton Trans.* **1998**, 2253.
(60) McInnes, J. M.; Swallow, D.; Blake, A. J.; Mountford, P. *Inorg. Chem.* **1998**, *37*, 5970.
(61) Kisko, J. L.; Hascall, T.; Parkin, G. *J. Am. Chem. Soc.* **1997**, *119*, 7609.
(62) Amgoune, A.; Thomas, C. M.; Roisnel, T.; Carpentier, J.-F. *Chem.−Eur. J.* **2006**, *12*, 169.
(63) Bonnet, F.; Cowley, A. R.; Mountford, P. *Inorg. Chem.* **2005**, *44*, 9046.
(64) Suzuki, Y.; Terao, H.; Fujita, T. *Bull. Chem. Soc. Jpn.* **2003**, *76*, 1493.
(65) Mitani, M.; Saito, J.; Ishii, S.; Nakayama, Y.; Makio, H.; Matsukawa, N.; Matsui, S.; Mohri, J.; Furuyama, R.; Terao, H.; Bando, H. H. T.; Fujita, T. *Chem. Rec.* **2004**, *4*, 137.
(66) Blake, A. J.; Collier, P. E.; Dunn, S. C.; Li, W.-S.; Mountford, P.; Shishkin, O. V. *J. Chem. Soc., Dalton Trans.* **1997**, 1549.
(67) Coles, M. P.; Dalby, C. I.; Gibson, V. C.; Clegg, W.; Elsegood, M. R. J. *Polyhedron* **1995**, *14*, 2455.
(68) Michelman, R. I.; Bergman, R. G.; Andersen, R. A. *Organometallics* **1993**, *12*, 2741.
(69) Pugh, S. M.; Clark, H. S. C.; Love, J. B.; Blake, A. J.; Cloke, F. G. N.; Mountford, P. *Inorg. Chem.* **2000**, *39*, 2001.
(70) Gade, L. H. Personal communication.

Scheme 1. Synthesis of Titanium Hydrazides Supported by Tridentate Diamide-Amine Ligands[a]

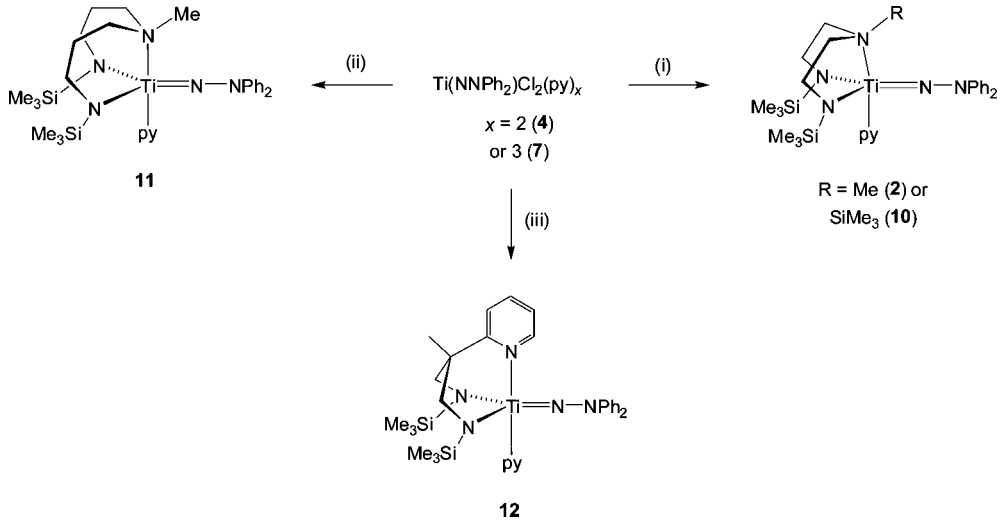

[a] Reagents and conditions: (i) $Li_2N_2N^{C_2,Me}$, −78 °C, toluene, 65% or $Li_2N_2N^{C_2,SiMe_3}$, −78 °C, toluene, 26%; (ii) $Li_2N_2N^{C_3,Me}$, −78 °C, toluene, 41%; (iii) $Li_2N_2N^{py}$, −78 °C, toluene, 73%.

Scheme 2. Synthesis of Titanium Hydrazides Supported by Tetradentate N_4- or O_2N_2-Donor Ligands[a]

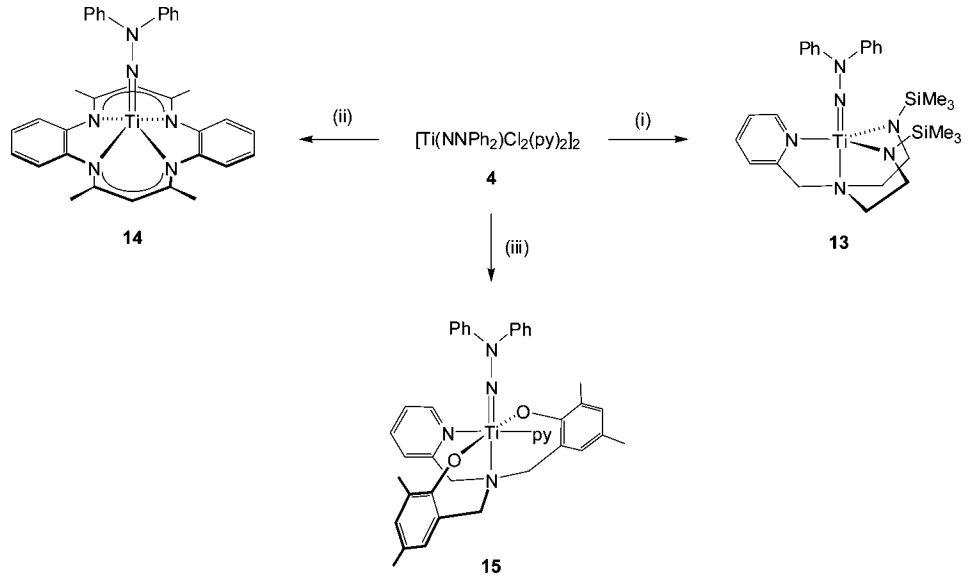

[a] Reagents and conditions: (i) Li_2N_2NN', −78 °C, toluene, 31%; (ii) Li_2Me_4taa, C_6D_6, 100%; (iii) Na_2O_2NN', −78 °C, toluene, 49%.

A wide number of titanium imido compounds[4,6] are available from synthons of the type $Ti(NR)Cl_2(py)_x$ or $Ti(NR)Cl_2(NHMe_2)_2$ (R = alkyl or aryl; $x = 2$ or 3)[66,71,72] by substitution strategies. We therefore considered an analogous approach for making new hydrazide complexes. At first sight, a suitable hydrazide synthon is $Ti(NNPh_2)Cl_2(NHMe_2)_2$ (prepared from $Ti(NMe_2)_2Cl_2$ and Ph_2NNH_2).[31] Unfortunately, the somewhat acidic N*H* groups of the $NHMe_2$ ligands lead to undesired side-reactions when the complexes are treated with anionic reagents such as lithiated amides.[4] However, the $NHMe_2$ ligands of $Ti(NNPh_2)Cl_2(NHMe_2)_2$ can be substituted by pyridine to form dimeric $[Ti(NNPh_2)Cl_2(py)_2]_2$ (**4**), believed to have terminal Ti=$NNPh_2$ groups and bridging Cl ligands.[31] Preliminary experiments showed that this material reacted with metalated salts of the target ligands to form the desired complexes in acceptable to good yields as described below (Schemes 1 and 2).

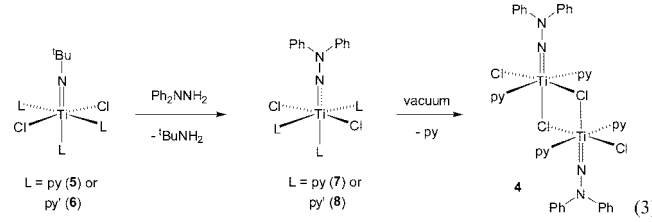

Although $[Ti(NNPh_2)Cl_2(py)_2]_2$ (**4**) can be prepared from $Ti(NNPh_2)Cl_2(NHMe_2)_2$, the latter itself requires at least a two-

(71) Adams, N.; Arts, H. J.; Bolton, P. D.; Cowell, D.; Dubberley, S. R.; Friederichs, N.; Grant, C.; Kranenburg, M.; Sealey, A. J.; Wang, B.; Wilson, P. J.; Cowley, A. R.; Mountford, P.; Schröder, M. *Chem. Commun.* **2004**, 434.

(72) Adams, N.; Bigmore, H. R.; Blundell, T. L.; Boyd, C. L.; Dubberley, S. R.; Sealey, A. J.; Cowley, A. R.; Skinner, M. E. G.; Mountford, P. *Inorg. Chem.* **2005**, *44*, 2882.

(73) Lorber, C.; Choukroun, R.; Donnadieu, B. *Inorg. Chem.* **2002**, *41*, 4217.

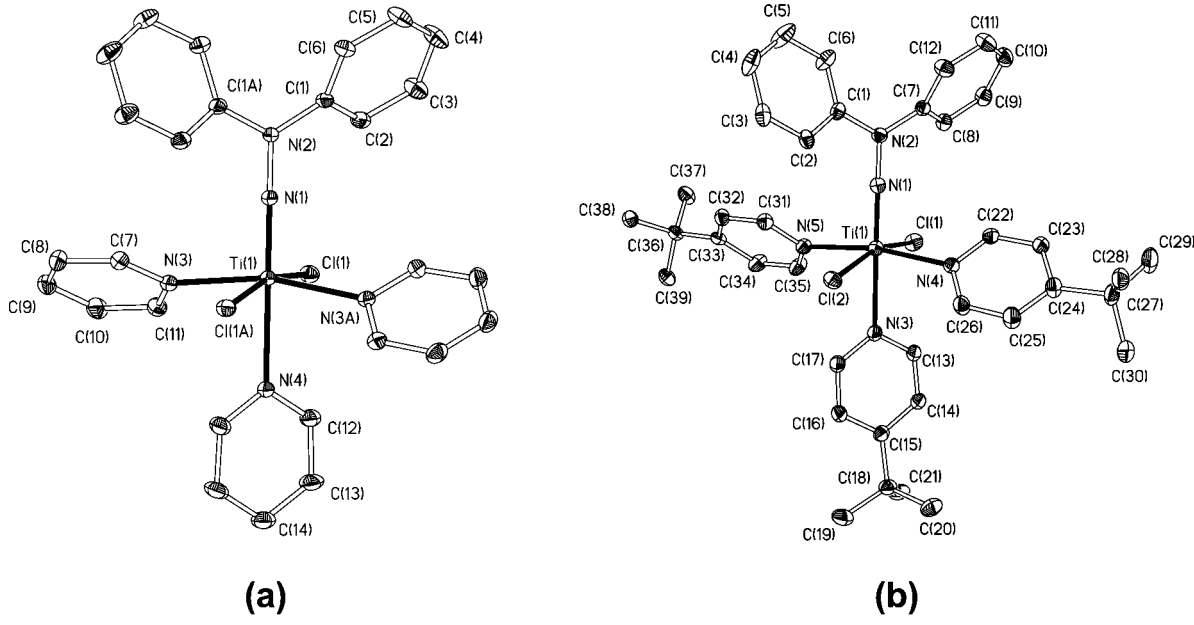

Figure 1. Displacement ellipsoid plots (25% probability) with H atoms omitted for clarity. (a) $Ti(NNPh_2)Cl_2(py)_3$ (**7**), atoms carrying the suffix "A" are related to their counterparts by the symmetry operator $-x+1, y, -z+{}^3/_2$. (b) One of the two crystallographically independent molecules of $Ti(NNPh_2)Cl_2(py')_3$ (**8**), second orientation of one of the py′ *tert*-butyl groups omitted.

step synthesis, and its conversion to **4** requires heating in a large excess of neat pyridine at 70 °C for 16 h, giving variable yields and purity. Similar difficulties with this type of apparently straightforward reaction have been noted for the imido systems $M(NR)Cl_2(NHMe_2)_2$ (M = Ti[72] or V[73]). We therefore developed an alternative route (eq 3) to **4** and well-defined monomeric homologues starting from the *tert*-butyl imido compounds $Ti(N^tBu)Cl_2(L)_3$ (L = py (**5**) or 4-$NC_5H_4{}^tBu$ (py′, **6**)). These are both readily available in multigram quantities from inexpensive and commerically available starting materials ($TiCl_4$, $^tBuNH_2$, and py or py′).[66,74]

Reaction of **5** with Ph_2NNH_2 (1 equiv) in benzene at room temperature overnight afforded a precipitate of bright yellow, monomeric $Ti(NNPh_2)Cl_2(py)_3$ (**7**) in 89% yield (ca. 5 g scale) and in analytically pure form. The corresponding reaction of **6** gave the homologous compound $Ti(NNPh_2)Cl_2(py')_3$ (**8**) in 74% yield, again as a pure yellow solid. The lower isolated yield for **8** reflects its higher solubility in hydrocarbon solvents. Further exposure of **7** to a dynamic vacuum leads to loss of one coordinated pyridine and eventual quantitative formation of the bis(pyridine) complex **4**. Analogous behavior is found for the imido systems $Ti(NR)Cl_2(py)_3$ (R = ^{t}Bu or aryl)[66] and was attributed to the strong labilizing effect of the imido groups on the pyridine *trans* to the Ti═NR bond.[75] Compound **8** does not easily lose the *trans* py′ ligand in this way because of the lower volatility of the substituted pyridine and its better donor ability. Both **4** and **7** were subsequently used as synthons for the syntheses described below, and there is no difference in their performance. Compound **8** was not used further in the present syntheses because preliminary studies found the parent pyridine adduct products were already very soluble and prone to be oily in some instances (due to the presence of $SiMe_3$ groups in the diamide complexes). Unfortunately, reaction of Me_2NNH_2 with **5** did not give terminal hydrazido compounds but only the hydrazide-bridged dimer $Ti_2(\mu\text{-}\eta^2,\eta^1\text{-}NNMe_2)_2Cl_4(py)_2$, which we found to be ineffective as a synthon.[31]

Table 1. Selected Bond Distances (Å) and Angles (deg) for $Ti(NNPh_2)Cl_2(py)_3$ (7)[a]

Ti(1)−N(1)	1.727(2)	Ti(1)−Cl(1)	2.4265(5)
Ti(1)−N(3)	2.2464(17)	Ti(1)−N(4)	2.402(2)
N(1)−N(2)	1.359(3)	N(2)−C(1)	1.411(2)
N(1)−Ti(1)−N(3)	97.25(4)	Cl(1)−Ti(1)−Cl(1A)	166.52(3)
N(1)−Ti(1)−Cl(1)	96.738(15)	Ti(1)−N(1)−N(2)	180
N(1)−Ti(1)−N(4)	180	N(1)−N(2)−C(1)	118.66(11)
N(3)−Ti(1)−Cl(1)	90.44(5)	C(1)−N(2)−C(1A)	118.66(11)

[a] Atoms carrying the suffix "A" are related to their counterparts by the symmetry operator $-x+1, y, -z+{}^3/_2$.

The NMR spectra of **7** and **8** show resonances for a $NNPh_2$ ligand and two py (or py′) ligand environments in a 2:1 ratio. The lower intensity py or py′ resonances are shifted upfield from their counterparts and are assigned to the ligands *trans* to the Ti═$NNPh_2$ functional groups. The solution NMR and other analytical data are fully consistent with the structures proposed in eq 3, but do not uniquely define them as monomeric terminal hydrazides. They have therefore been characterized by X-ray crystallography in both cases. The molecular structures are shown in Figure 1, and key distances and angles are given in Tables 1 and 2. Molecules of **7** lie on crystallographic 2-fold rotation axes passing through the Ti(1)−N(1)−N(2) linkage, while compound **8** contains two crystallographically independent molecules in the asymmetric unit. Some positional disorder of certain py′ *tert*-butyl groups of **8** was satisfactorily modeled.

The structures of **7** and **8** confirm those anticipated in eq 3. These are only the second and third examples of a structurally authenticated Ti═$NNPh_2$ functional group (two such examples are now known for zirconium).[29,35] The other titanium example is $Ti(NNPh_2)\{HC(Me_2pz)_3\}Cl_2$ (**9**), which also contains an octahedral Ti, but with *fac*-coordination of the N_3-donor set and mutually *cis* Cl ligands. Since a number of imido analogues $Ti(NR)Cl_2(py)_3$ (R = ^{t}Bu or aryl) have been structurally characterized,[23,24] **7** and **8** provide an excellent opportunity for

(74) Dunn, S. C.; Batsanov, A. S.; Mountford, P. *J. Chem. Soc., Chem. Commun.* **1994**, 2007.
(75) Kaltsoyannis, N.; Mountford, P. *J. Chem. Soc., Dalton Trans.* **1999**, 781.

Table 2. Selected Bond Distances (Å) and Angles (deg) for $Ti(NNPh_2)Cl_2(py')_3$ (8)[a]

Ti(1)−N(1)	1.7240(18)	[1.7216(17)]	Ti(1)−N(5)	2.2274(18)	[2.211(2)]
Ti(1)−Cl(1)	2.4079(7)	[2.4132(7)]	N(1)−N(2)	1.351(2)	[1.353(2)]
Ti(1)−Cl(2)	2.4224(7)	[2.3967(6)]	N(2)−C(1)	1.414(3)	[1.423(3)]
Ti(1)−N(3)	2.3942(19)	[2.483(2)]	N(2)−C(7)	1.430(3)	[1.417(3)]
Ti(1)−N(4)	2.2417(18)	[2.2314(19)]			
N(1)−Ti(1)−N(3)	178.56(8)	[178.20(8)]	N(4)−Ti(1)−N(5)	169.51(7)	[172.69(7)]
N(1)−Ti(1)−N(4)	94.51(8)	[93.71(8)]	Ti(1)−N(1)−N(2)	179.54(15)	[178.38(16)]
N(1)−Ti(1)−N(5)	95.97(8)	[93.41(8)]	N(1)−N(2)−C(1)	118.49(17)	[117.77(18)]
N(1)−Ti(1)−Cl(1)	96.68(6)	[98.30(6)]	N(1)−N(2)−C(7)	118.69(17)	[118.54(18)]
N(1)−Ti(1)−Cl(2)	99.23(6)	[98.23(6)]	C(1)−N(2)−C(7)	122.82(17)	[123.45(18)]
Cl(1)−Ti(1)−Cl(2)	164.07(3)	[163.43(3)]			

[a] Values in brackets are for the other crystallographically independent molecule.

structural comparisons with their better established imido analogues.

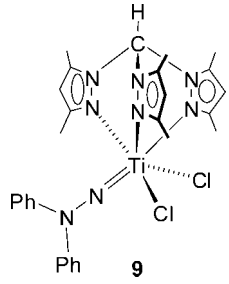

9

The metric data for the structures of **7** and **8** are generally comparable within error. They possess pseudo-octahedral geometries at Ti(1), mutually *trans* Cl donors, and three py (or py′) ligands arranged in a *mer* fashion. This is the same as for the imido analogues $Ti(NR)Cl_2(py)_3$.[23,24] There is a significant bond-lengthening effect of the hydrazido ligand on the py or py′ ligand opposite it, and the magnitude of this *trans* influence (av ca. 0.20 Å) is comparable to that found in the imido analogues. The Ti−Cl and Ti−py (py′) distances for **7** and **8** are within the ranges found for these imido and other Ti(+4) compounds.[23,24] They are thus consistent with $NNPh_2$ acting as a formally dianionic "hydrazide(2−)" ligand (as opposed to being considered as a neutral $N{=}NPh_2$ "isodiazene"[76]) in these titanium complexes, as also found in the DFT calculations for **9**.[31]

The parameters associated with $Ti{=}NNPh_2$ linkages are similar to those in **9** with comparable $Ti{=}N_\alpha$ (1.722(2)−1.727(2) Å) and $N_\alpha{-}N_\beta$ (1.351(2)−1.359(3) Å) distances (cf. 1.718(2) and 1.369(3) Å, respectively in **9**). Likewise, the hydrazide linkages are linear ($Ti{=}N{-}NPh_2$ = 178−180 °) and the N_β nitrogen is planar (sum of the angles subtended at N(2) ∼360 ° within error) for both compounds. The Ph rings are rotated by ca. 30−40° out of the plane containing the $Ti{=}N{-}N(C_{ipso})_2$ atoms, and the $N_\beta{-}C_{ipso}$ distances are approximately equivalent in all cases (1.41−1.42 Å). This suggests the possibility of partial delocalization of electron density from the sp^2-hybridized N_β onto the phenyl rings.

The $Ti{=}N_\alpha$ distances in **7** and **8** are all slightly longer than for the imido complexes $Ti(NR)Cl_2(py)_3$: R = ^{t}Bu, Ti=N = 1.705(3) Å; R = Ph, 1.714(2) Å; R = *p*-Tol, 1.705(4) Å).[66] They are, however, well within the general range (ca. 1.68−1.76 Å based on titanium imides) expected for a formal $Ti{\equiv}N_\alpha$ triple bond ($\sigma^2\,\pi^4$). This triple-bond assignment is also consistent with previous DFT calculations on **9** and also the observed linear $Ti{=}N{-}NPh_2$ linkage (sp-hybridized N_α).[31] In contrast, the average $N_\alpha{-}N_\beta$ distance for transition metal diphenylhydrazido compounds in general is 1.317 Å,[23,24] and so in this sense the $N_\alpha{-}N_\beta$ distances for **7** and **8** are comparatively long.

Synthesis of Titanium Hydrazides Containing Dianionic N_3-, N_4-, and O_2N_2-Donor Ligands. As mentioned, both $[Ti(NNPh_2)Cl_2(py)_2]_2$ (**4**) and $Ti(NNPh_2)Cl_2(py)_3$ (**7**) serve as starting materials for the general synthesis of new families of titanium diphenyl hydrazides containing dianionic N_3- and N_4-donor ligands. The syntheses are summarized in Schemes 1 and 2.

Preliminary studies focused on the $N_2N^{C_2,SiMe_3}$ ligand system, which we have previously used in the *tert*-butyl imido complex $Ti(N^tBu)(N_2N^{C_2,SiMe_3})(py)$. Reaction of $Li_2N_2N^{C_2,SiMe_3}$ with **4** in benzene at room temperature gave the crude product as a green-brown solid. The ^{1}H NMR spectrum showed the presence of both the desired complex $Ti(NNPh_2)(N_2N^{C_2,SiMe_3})(py)$ (**10**) and free protio-ligand $H_2N_2N^{C_2,SiMe_3}$ in a ca. 1:2 ratio. The presence of $H_2N_2N^{C_2,SiMe_3}$ is attributed to redox-coupled H atom abstraction side-reactions, as have been found previously in some analogous reactions of this ligand.[69] These could be partially alleviated by starting the reaction at −78 °C and adding precooled toluene to a cold solid mixture of $Li_2N_2N^{C_2,SiMe_3}$ and **4**, followed by a short reaction time and workup. Analytically pure samples of **10** were obtained in 26% overall yield, the relatively high solubility of **10** in hydrocarbon solvents also contributing to the disappointing yield.

The reactions between **4** and $Li_2N_2N^{C_2,Me}$ or $Li_2N_2N^{C_3,Me}$ were carried out in the same way and afforded the homologous complexes $Ti(NNPh_2)(N_2N^{C_23,Me})(py)$ (**2**) and $Ti(NNPh_2)(N_2N^{C_3,Me})(py)$ (**11**) in 65% and 41% isolated yield. We found that $Li_2N_2N^{py}$ reacted smoothly with **4** to form $Ti(NNPh_2)(N_2N^{py})(py)$ (**12**) in good yield (73%) without noticeable redox complications. This reaction could best be performed by adding a cold solution of the lithiated amide to **4**. The NMR and other analytical data for the new compounds **10**−**12** are fully consistent with the structures proposed in Scheme 1, which have all been confirmed by X-ray crystallography (*vide infra*).

We were also interested to prepare complexes with dianionic N_4-donor ligands (Scheme 2). Thus reaction of Li_2N_2NN' with **4** under analogous conditions for **2**, **10**, and **11** afforded the five-coordinate $Ti(NNPh_2)(N_2NN')$ (**13**). We were not able to grow diffraction-quality crystals of **13**, but its NMR data are consistent with the C_s symmetrical, trigonal-bipyramidal structure proposed in Scheme 2. Titanium and zirconium imido analogues of **13** have been reported previously and have comparable structures.[77] The chemical shift of the *ortho*-H of the pyridyl donor in **13** appears at δ 8.98 ppm, consistent with it being coordinated in solution (in free H_2N_2NN' this hydrogen

(76) Kahlal, S.; Saillard, J.-Y.; Hamon, J.-R.; Manzur, C.; Carrillo, D. *J. Chem. Soc., Dalton Trans.* **1998**, 1229.

(77) Skinner, M. E. G.; Toupance, T.; Cowhig, D. A.; Tyrrell, B. R.; Mountford, P. *Organometallics* **2005**, *24*, 5586.

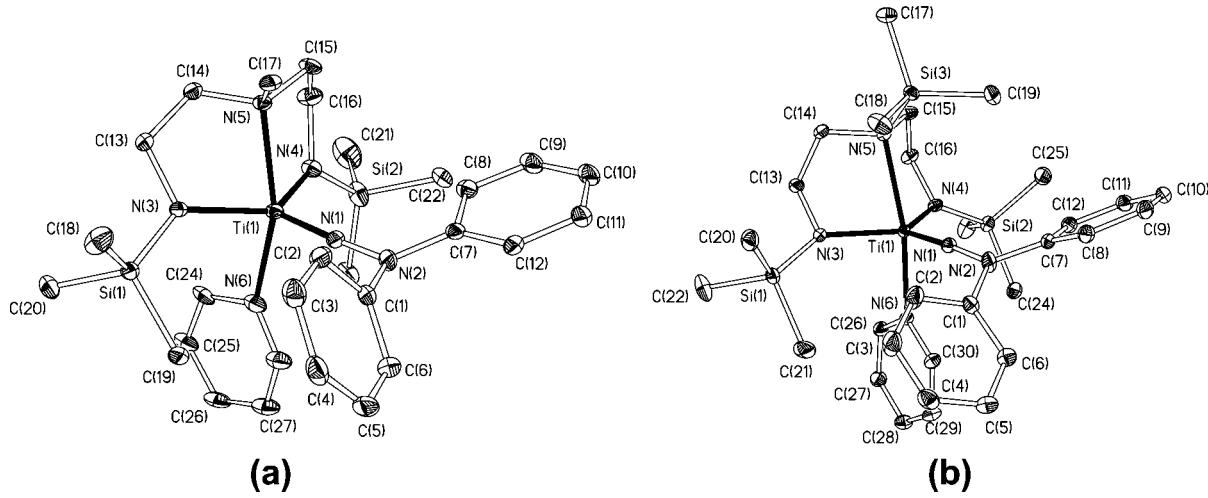

Figure 2. Displacement ellipsoid plots with H atoms omitted for clarity. (a) $Ti(NNPh_2)(N_2N^{C_2,Me})(py)$ (**2**, 20% probability, disorder in coordinated pyridine omitted). (b) $Ti(NNPh_2)(N_2N^{C_2,SiMe_3})(py)$ (**10**, 30% probability).

appears at δ 8.60 ppm).[78] Significantly, **13** is the neutral group 4 analogue of Schrock's triamide-amine (tren)-supported Mo−NNR_2 (R = alkyl or H) systems.[10,20,79]

As mentioned, $Ti(NNPh_2)(Me_4taa)$ (**14**) was previously prepared by reaction of $Ti(N^tBu)(Me_4taa)$ with Ph_2NNH_2.[39] As shown in Scheme 2, the reaction between Li_2Me_4taa and **4** in C_6D_6 gave quantitative conversion to **14** immediately at room temperature, indicating this is a viable route to macrocycle-supported hydrazides also. The NMR data for **14** were comparable to those of an authentic sample prepared by the original imide/hydrazine exchange route.

We have also made a comparison between the N_4-donor systems $Ti(NNPh_2)(L)$ (L = N_2NN' (**13**) or Me_4taa (**14**)) and those of O_2NN' (see Chart 1) as a representative bis(phenolate)-diamine ligand. Addition of a cold toluene solution of Na_2O_2NN' to $[Ti(NNPh_2)Cl_2(py)_2]_2$ (**4**) gave the compound $Ti(NNPh_2)(O_2NN')(py)$ (**15**) in 49% yield as summarized in Scheme 2. The NMR data for **15** are consistent with the C_s symmetric structure proposed and confirm the presence of the coordinated pyridine. Corresponding monomeric titanium imido complexes of O_2NN'-type ligands have been prepared previously.[80] Unfortunately we have not been able to obtain diffraction-quality crystals of **15**, and for the remainder of this paper we shall focus on the diamide-amine systems. Attempts to prepare a terminal dimethyl hydrazide analogue of **15** are described in the Supporting Information along with the X-ray structure of dimeric $Ti_2(\mu\text{-}\eta^2\eta^1\text{-}NNMe_2)_2(O_2NN')_2$ (**16**).

Structures of Titanium Hydrazides Containing N_3-Donor Ligands. The compounds **2** and **10**−**12** offer an excellent opportunity to determine systematically the effects of the different diamide-amine ligands on the ground-state structure of this new class of titanium hydrazide complexes, and thereby gain insight into the unique reactivity of these systems. Diffraction-quality crystals of $Ti(NNPh_2)(N_2N^{C_2,Me})(py)$ (**2**), $Ti(NNPh_2)(N_2N^{C_2,SiMe_3})(py)$ (**10**), $Ti(NNPh_2)(N_2N^{C_3,Me})(py)$ (**11**), and $Ti(NNPh_2)(N_2N^{py})(py)$ (**12**) were grown from the appropriate solvents. The molecular structures are shown in Figures 2 (**2**, **10**) and 3 (**11**, **12**). Key bond distances and angles are compared in Table 3.

All four complexes possess trigonal-bipyramidal titanium centers with the diamide-amine ligand coordinating in a *fac* manner. The hydrazide N(1) (N_α) and amide nitrogens (N(3), N(4)) occupy the equatorial positions of the trigonal bipyramids; the neutral donors, the axial sites. The Ti−N and intraligand distances and angles for the diamide-amine and pyridine donors are all within the expected ranges,[23,24] although there are some interesting variations as discussed below. The titanium *tert*-butyl imido analogues of **10** and **12** have been reported previously,[69,81] as have related group 4 and 5 imido complexes Zr(N-2,6-$C_6H_3{}^iPr_2)(N_2N^{py})$(py) and $Ta(N^tBu)(N_2N^{py})Cl$.[81,82] These have comparable structures with the amide and imide nitrogens in the equatorial plane. In the hydrazide structures, as in the aforementioned imido complexes, the amide nitrogens are trigonal planar (sum of the angles subtended at N(3) and N(4) = 360° within error) and sp^2 hybridized, which is typical for early transition metal complexes.[50,54]

Before considering the data associated with the Ti=$NNPh_2$ moieties it is necessary to examine more closely the variations in the $Ti(N_2N^R)(py)$ fragments in the four complexes. The five-membered chelate rings formed by the diamide-amine ligands in **2** and **10** lead to larger N(1)−Ti(1)−N(5) angles (av ca. 103°) compared to those for **11** and **12** (six-membered chelate rings, av ca. 94°), thus pulling the apical donor away from the Ti=$NNPh_2$ linkage. The N(5)−Ti(1)−N(6) angles are correspondingly smaller for **2** and **10** (av ca. 161°) than for **11** and **12** (av ca. 173°). This in turn affects the Ti(1)−N(6) bond distances for the pyridine ligand (shorter in **2** and **10** (av ca. 2.22 Å) than in **11** and **12** (av ca. 2.27 Å). The effect of replacing the apical N-Me of the diamide ligand in **2** with the bulky N-$SiMe_3$ in **10** results in a 0.131(4) Å lengthening of the Ti(1)−N(5) bond. Interestingly, the Ti(1)−N(6) distances for the pyridine ligands do not vary significantly between **2** and **10** (difference 0.011(5) Å). Finally it is important to note that the variations in the diamide-amine ligand framework lead to significant changes in the Ti(1)−N(3) and Ti(1)−N(4) distances to the amide nitrogens. Thus from **2** to **12** the average Ti−N_{amide}

(78) Skinner, M. E. G.; Li, Y.; Mountford, P. *Inorg. Chem.* **2002**, *41*, 1110.
(79) O'Donoghue, M. B.; Davis, W. M.; Schrock, R. R. *Inorg. Chem.* **1998**, *37*, 5149.
(80) Boyd, C. L.; Toupance, T.; Tyrrell, B. R.; Ward, B. D.; Wilson, C. R.; Cowley, A. R.; Mountford, P. *Organometallics* **2005**, *24*, 309.
(81) Blake, A. J.; Collier, P. E.; Gade, L. H.; Mountford, P.; Lloyd, J.; Pugh, S. M.; Schubart, M.; Skinner, M. E. G.; Trösch, J. M. *Inorg. Chem.* **2001**, *40*, 870.
(82) Ward, B. D.; Orde, G.; Clot, E.; Cowley, A. R.; Gade, L. H.; Mountford, P. *Organometallics* **2004**, *23*, 4444.

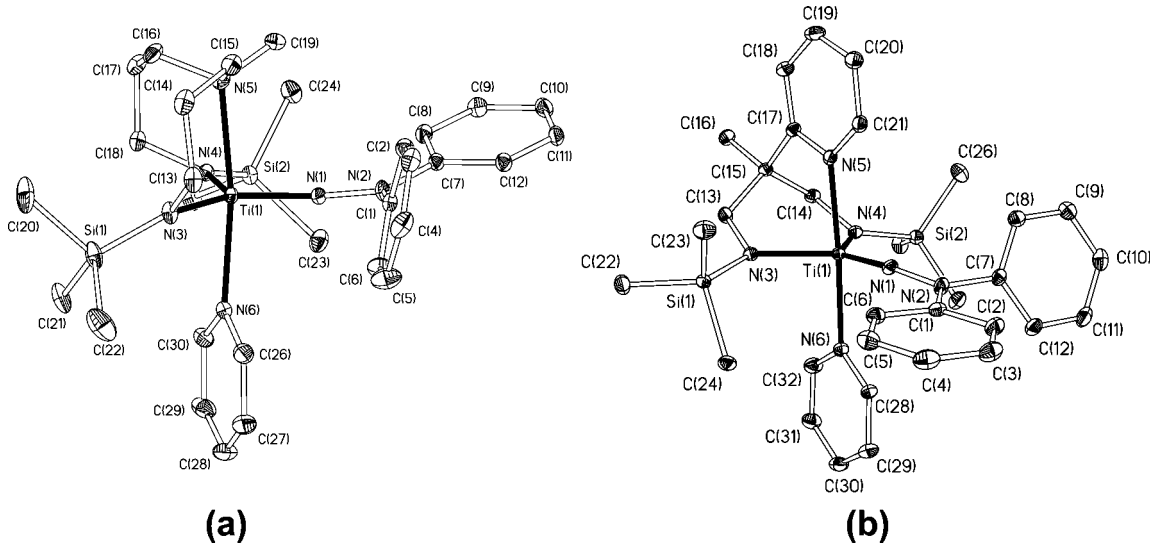

Figure 3. Displacement ellipsoid plots with H atoms omitted for clarity. (a) $Ti(NNPh_2)(N_2N^{C_3,Me})(py)$ (**11**, 20% probability, minor disorder omitted). (b) $Ti(NNPh_2)(N_2N^{py})(py)$ (**12**, 20% probability).

Table 3. Selected Bond Distances (Å) and Bond and Torsion Angles (deg) for $Ti(NNPh_2)(N_2N^{C_2,Me})(py)$ (2), $Ti(NNPh_2)(N_2N^{C_2,SiMe_3})(py)$ (10), $Ti(NNPh_2)(N_2N^{C_3,Me})(py)$ (11), and $Ti(NNPh_2)(N_2N^{py})(py)$ (12)[a]

parameter	2	10	11	12
Ti(1)−N(1)	1.733(5)	1.750(2)	1.7506(14)	1.759(2)
Ti(1)−N(3)	2.029(5)	2.014(2)	1.999(2)	1.974(2)
Ti(1)−N(4)	2.026(5)	2.003(2)	2.0020(14)	1.974(2)
Ti(1)−N(5)	2.224(4)	2.355(2)	2.289(2)	2.184(2)
Ti(1)−N(6)	2.215(5)	2.226(2)	2.281(2)	2.259(2)
N(1)−N(2)	1.359(7)	1.362(2)	1.364(2)	1.367(2)
N(2)−C(1)	1.438(7)	1.426(2)	1.433(2)	1.393(3)
N(2)−C(7)	1.399(7)	1.403(2)	1.398(2)	1.434(3)
N(1)−Ti(1)−N(3)	113.8(2)	118.83(7)	114.89(6)	124.52(8)
N(1)−Ti(1)−N(4)	113.7(2)	120.57(7)	116.03(6)	128.74(8)
N(3)−Ti(1)−N(4)	130.5(2)	120.29(7)	128.98(6)	106.64(7)
N(1)−Ti(1)−N(5)	102.1(2)	104.01(6)	92.91(6)	95.49(7)
N(1)−Ti(1)−N(6)	99.3(2)	93.17(7)	95.57(6)	90.25(7)
N(5)−Ti(1)−N(6)	158.4(2)	162.82(6)	171.49(5)	174.26(6)
Ti(1)−N(1)−N(2)	177.7(4)	173.22(14)	168.75(13)	163.8(2)
N(1)−N(2)−C(1)	116.1(4)	118.3(2)	116.78(14)	121.2(2)
N(1)−N(2)−C(7)	120.9(5)	120.2(2)	121.25(14)	115.9(2)
C(1)−N(2)−C(7)	119.5(5)	121.4(2)	120.66(14)	122.7(2)
av N(1)−Ti(1)−N(3)−R^1	53.0	38.6	37.4	21.2
av N(1)−Ti(1)−N(4)−R^2	70.3	49.4	21.5	25.2

[a] "Av N(1)−Ti(1)−N(3,4)−$R^{1,2}$" refers to the average of the torsion angles N(1)−Ti(1)−N(3,4)−Si or N(1)−Ti(1)−N(3,4)−C for the linkages under consideration.

distance decreases from ca. 2.027 Å to 1.974 Å. At the same time the orientation of the amide nitrogen substituents relative to the equatorial plane changes such that they become more coplanar with the amide nitrogens and hydrazide N_α. This can be quantified by the average N(1)−Ti(1)−N_{amide}−R torsion angles (see Table 3), which decrease from 61.6° in **2** to 23.2° in **12**. The significance of these variations is evaluated using DFT later.

Turning now to the $Ti{=}NNPh_2$ moiety, it is seen that in all compounds the Ti(1)−N(1)−N(2) linkage is approximately linear (163.8(2)−177.7(4)°). The β-nitrogen (N(2)) is effectively trigonal planar, as judged by the sums of the angles subtended at this atom (range 356(1)−360(1)°). These features are also consistent with the structures of **7**, **8**, and **9**. Similarly, the N(1)−N(2) distances in **2** and **10**−**12** (1.359(7)−1.367(2) Å) fall within the range of those found in the dichloride complexes (range 1.351(2)−1.369(3) Å). In contrast, the Ti(1)−N(1) distances (1.733(5)−1.759(2) Å) are systematically longer than for **7**, **8**, and **9** (range 1.718(2)−1.727(2) Å). The same situation is found when comparing the $Ti{=}N^tBu$ distances of $Ti(N^tBu)(N_2N^{C_2,SiMe_3})(py)$[69] and $Ti(N^tBu)(N_2N^{py})(py)$[81] with that of $Ti(N^tBu)Cl_2(py)_3$[66] and in the first instance can be attributed to the good donor abilities of diamide-amine ligands. The $Ti{=}N_\alpha$ distances in **10** and **12** are longer by 0.032(4) and 0.035(3) Å than the $Ti{=}N^tBu$ distances in the corresponding imido complexes, as expected from our earlier comparison of **7** with $Ti(N^tBu)Cl_2(py)_3$.

The N_β−C_{ipso} distances (N(2)−C(1) and N(2)−C(7)) merit comment. In **10** the difference between them is relatively small (0.023(3) Å), and the phenyl groups are twisted out of the {N(2),C(1),C(7)} least-squares plane by ca. 27° and 47° for C(7) and C(1), respectively. In the other structures the differences between the N_β−C_{ipso} distances are significantly larger (0.035(3)−0.041(4) Å), and at the same time the differences in the extent of twisting of the phenyl rings out of the {N(2),N(1),N(7)} planes become much larger. In **2**, **11**, and **12** one phenyl ring is much more coplanar (twist angle 4−9°) than the other (twist angle 47−69°). The more coplanar phenyl rings are associated with the shorter N_β−C_{ipso} distances (range 1.393(3)−1.399(7) Å, cf. 1.433(2)−1.438(7) Å). These trends are evidence for efficient π conjugation between N_β and the phenyl substituents.[83] Previous *ab initio* calculations have found that the free model hydrazide dianion $[NNH_2]^{2-}$ has a pyramidalized β-nitrogen, as does the monoanion and the triplet form of neutral NNH_2.[76] In contrast, the formally dianionic[31] $NNPh_2$ groups in group 4 systems possess planar β-nitrogens. Since terminal $Ti{=}NNMe_2$ analogues feature pyramidal β-Ns,[30,34] it appears that the planarity of the diphenyl hydrazide β-nitrogens is due to N_β−C_{ipso} conjugation.

It is interesting to note the variation in Ti(1)−N(1), N(1)−N(2), and Ti(1)−N(1)−N(2) parameters on going from **2** to **12** (Table 3). There is an apparent trend in lengthening of both the Ti(1)−N(1) and N(1)−N(2) distances and a decrease in the Ti(1)−N(1)−N(2) angle along this series. At the same time, as mentioned above, the diamide-amine Ti(1)−N(3) and Ti(1)−N(4) distances are decreasing, and the amide nitrogen substituents are becoming more coplanar with the {Ti(1),N(1),N(2),N(3)}

(83) Either strongly to just one Ph ring (e.g., **2**, **11**, **12**) or in an intermediate way to both (e.g., **7**, **8**, **10**)

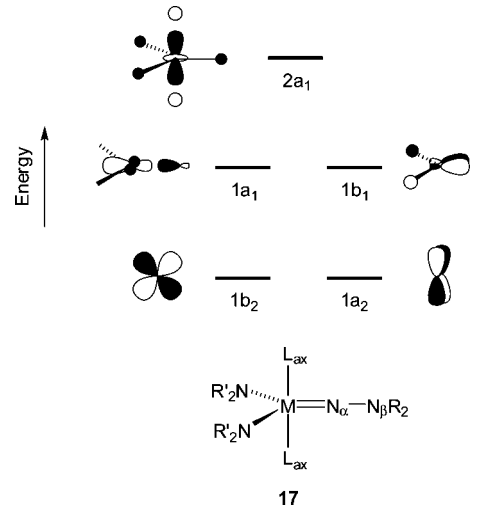

17

Figure 4. σ-Only frontier MOs (d orbitals only, arbitrary energies) for hypothetical bis(dialkylamide)-hydrazide system **17**. Labels are for C_{2v} symmetry, and L_{ax} represents a nominal axial ligand.[81,82]

trigonal plane. In contrast, the orientation of the $N_\beta Ph_2$ moiety is preserved in all these compounds, with the {N(1),N(2),C(1),C(7)} least-squares plane being effectively coplanar with {Ti(1),N(1), N(2),N(3)} in all instances. To help account for these observations and to gain a better understanding of their bonding in general, we analyzed the competition between the amide and hydrazide nitrogen π-donor orbitals for the Ti(d_π) acceptor MOs and considered how this would be affected by the orientation of the various amide N and hydrazide N_β substituents.

Molecular Orbital Analysis of Titanium Hydrazides Containing Dianionic N_3-Donor Ligands. We have previously reported detailed analyses of the metal(d_π)−N(p_π) bonding in d^0 imido complexes of the type $M(N_2N^{py})(NR)(L)$ (L = σ donor).[81,82] This serves as a starting point for considering the π-bonding situation in **2** and **10**−**12**. Figure 4 illustrates the σ-only frontier MOs (d orbitals only, arbitrary energies) for a hypothetical trigonal-bipyramidal complex $M(NNR_2)(NR'_2)_2(L_{ax})_2$ (**17**), where L_{ax} is a σ-only donor. The $2a_1$ MO is strongly σ^* antibonding and would not engage in metal−ligand π interactions. The $1a_1$ and $1b_1$ levels are slightly σ^* metal−ligand antibonding and higher in energy than the strictly σ-nonbonding $1b_2$ and $1a_2$ levels. Although these four orbitals are all available for metal−ligand π-bonding interactions with correctly oriented amide and hydrazide p_π donors, the $1b_2$ and $1a_2$ levels are the acceptors with the best energy match.

Figure 5a shows schematically the four highest occupied MOs of a planar, dianionic $[NNR_2]^{2-}$ ligand based on previous EHMO and DFT calculations.[27,31,76,84] The $1a_1$ MO is suitable for M−N_α σ bonding, and the $1b_2$ MO is N_α−N_β π bonding and would not be expected to interact to any significant extent with a metal center.[31,76] The $1b_1$ MO (which we abbreviate as π_h) is essentially N_α−N_β nonbonding and would form one of the M−N_α π bonds. The $2b_2$ MO (abbreviated π_v) is the HOMO of $[NNR_2]^{2-}$ and lies significantly higher in energy ($\geq$1 eV[31,76]) than the $1b_1$ MO because of its N_α−N_β π^*-antibonding nature. Of these two MOs (π_v ($2b_2$) and π_h ($1b_1$)), the former is the better π donor due to its better energy match with the metal acceptor orbitals. Donation of electron density from the π_v strengthens the N_α−N_β bond due to the formal removal of π^*-antibonding electron density. The consistent orientation of the $N_\beta Ph_2$ moiety in **2**−**12** is therefore understood in terms of providing the best interaction between the NNR_2 and titanium since this provides the most favorable overlap between the highest energy donor MO of $NNPh_2$ ($2b_2$) and the appropriate lowest energy acceptor orbital at titanium ($1b_2$ in Figure 4). The second π interaction between Ti and N_α is formed between the $1b_1$-donor MO of $NNPh_2$ and the $1b_1$ acceptor at the metal center.

The trigonal planar amide nitrogens of the real compounds **2** and **10**−**12** suggest that they are able in principle to donate two electrons each from the occupied $2p_\pi$ AOs (giving each complex an 18 valence electron count). However, as discussed previously,[81,82] the situation is complicated by symmetry restrictions, the details of which depend on the orientation of the lone pairs with respect to the equatorial plane of the complex. In the model complex **17** two extreme positions can be identified as depicted in Figure 5b,c. In Figure 5b the lone pairs are lying in the equatorial plane and their orientation is defined by a dihedral angle N_α−Ti−N−R′ of 90°. In Figure 5c the lone pairs are perpendicular to the equatorial plane and the dihedral angle N_α−Ti−N−R′ is 0°. In both cases it can be seen that one of the amide SALCs competes with one of the NNR_2 MOs of the corresponding symmetry for the same π-acceptor orbital at the metal center. This is either the $1b_1$ orbital in the case of Figure 5b or the $1b_2$ orbital when the amide SALCs are oriented as in Figure 5c. Thus in either extreme (and at all points in between) there is always a three-center−four-electron π-bonding conflict, and so the real complexes are best described as 16 valence electron "π-loaded" systems. This type of situation is well established in imido chemistry with very interesting consequences for metal−ligand multiple bonding properties and reactivity patterns.[1,81,82,85−90]

To test these qualitative ideas, the structure of $Ti(NNPh_2)(N_2N^{C_2,Me})(py)$ (**2**) has been optimized using DFT. The agreement between the computed (see Table S3 of the Supporting Information) and experimental geometries is very good. The four highest occupied MOs for **2** are shown in Figure 6. The orientation of the amide donors in **2** lies closer to the situation described by Figure 5b, and the appearance and energies of the HOMOs can be interpreted in terms of the qualitative model described above. The HOMO of **2** is the bonding combination between π_v of $NNPh_2$ and $1b_2$ on Ti and lies 1.9 eV above the corresponding π_h-derived orbital (HOMO−3). Both the HOMO and HOMO−3 are heavily ligand-based, and the $NNPh_2$ is best described as a hydrazido(2−) ligand forming a Ti−N_α triple bond. The very large destabilization of the HOMO is attributed to the N_α−N_β antibonding contribution. The LUMO of **2** is essentially the LUMO of pyridine with some weak bonding Ti−N interaction with a 3d AO on Ti.

The HOMO−3 also contains a minor contribution from the out-of-phase amide nitrogen lone pairs of the $N_2N^{C_2,Me}$ ligand (formally the b_1 SALC in Figure 5b), which is competing with π_h for the single suitable acceptor MO on titanium (equivalent

(84) Kahlal, S.; Saillard, J.-Y.; Hamon, J.-R.; Manzur, C.; Carrillo, D. *New J. Chem.* **2001**, *25*, 231.

(85) Green, J. C.; Green, M. L. H.; James, J. T.; Konidaris, P. C.; Maunder, G. H.; Mountford, P. *J. Chem. Soc., Chem. Commun.* **1992**, 1361.

(86) Dunn, S. C.; Mountford, P.; Robson, D. A. *J. Chem. Soc., Dalton Trans.* **1997**, 293.

(87) Parkin, G.; van Asselt, A.; Leahy, D. J.; Whinnery, L.; Hua, N. G.; Quan, R. W.; Henling, L. M.; Schaefer, W. P.; Santarsiero, B. D.; Bercaw, J. E. *Inorg. Chem.* **1992**, *31*, 82.

(88) Schofield, M. H.; Kee, T. P.; Anhaus, J. T.; Schrock, R. R.; Johnson, K. H.; Davis, W. M. *Inorg. Chem.* **1991**, *30*, 3595.

(89) Benson, M. T.; Bryan, J. C.; Burrell, A. K.; Cundari, T. R. *Inorg. Chem.* **1995**, *34*, 2348.

(90) Lin, Z.; Hall, M. B. *Coord. Chem. Rev.* **1993**, *123*, 149.

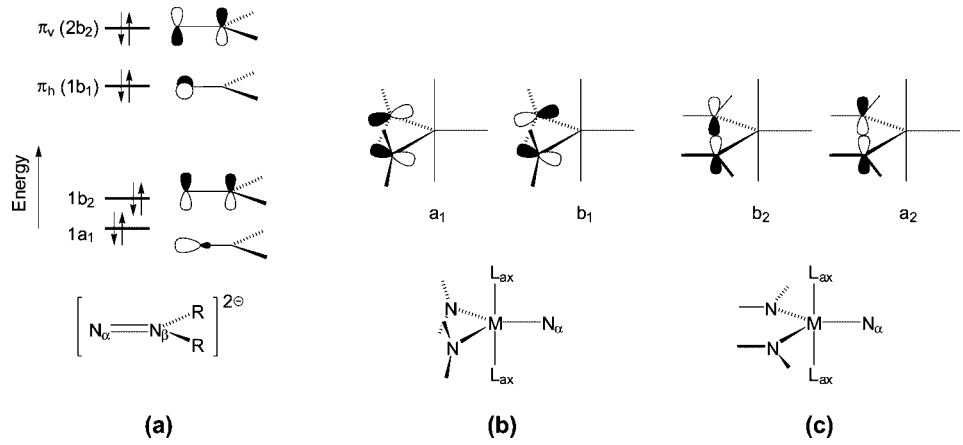

Figure 5. (a) Four highest occupied MOs of a C_{2v} symmetric dianion $[NNR_2]^{2-}$. (b) Amide lone pair SALCs when the lone pair 2p AOs lie in the equatorial plane. (c) Amide lone pair SALCs when the lone pair 2p AOs are perpendicular to the equatorial plane. Symmetry labels are given for the C_{2v} point group.

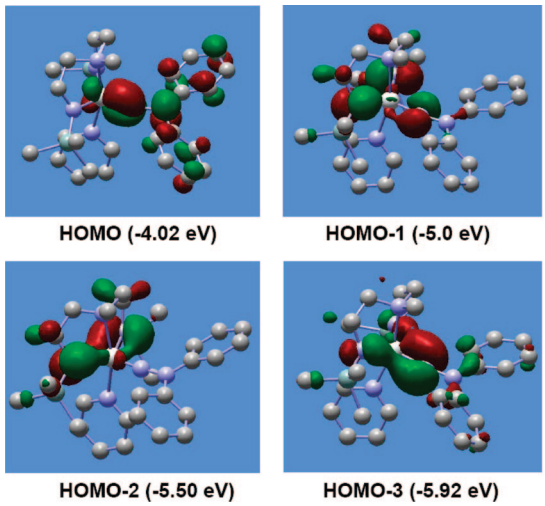

Figure 6. Four highest occupied MOs of $Ti(NNPh_2)(N_2NC_2,Me)(py)$ (**2**) and their DFT-computed energies.

to $1b_1$ in Figure 4). The HOMO−2 of **2** represents a $Ti-N_{amide}$ π-bonding interaction from the in-phase amide nitrogen lone pairs of $N_2N^{C_2,Me}$ (formally the a_1 SALC in Figure 5b), which does not compete with either π_v or π_h. The HOMO−1 is essentially a Ti−N nonbonding, ligand-based lone pair in nature. Its major contribution comes from the out-of-phase amide nitrogen lone pairs of $N_2N^{C_2,Me}$, although there is also a contribution from π_h. Therefore each amide nitrogen of $N_2N^{C_2,Me}$ is effectively a two-electron donor as a consequence of the π-loaded nature of **2**. It appears that π_h competes more effectively than the amide b_1 SALC for the single b_1-type acceptor orbital at titanium, consistent with the shorter $Ti-N_\alpha$ compared to $Ti-N_{am}$ bond distances (calculated values 1.735 and 2.015 (av) Å, respectively). However, the most remarkable feature of the bonding in **2** is the significant destabilization of the HOMO. This not only lies substantially above the other $Ti-N_\alpha$ π bond (HOMO−3) but is even ca. 1 eV above the nonbonding HOMO−1. The high energy of this MO (which is simultaneously $Ti-N_\alpha$ bonding and $N_\alpha-N_\beta$ antibonding) may be responsible for the very novel reactivity found between **2** and alkynes (eq 2).

NBO Analysis of Model Hydrazido and Imido Complexes. As mentioned, **2** lies closer to the situation in Figure 5b with the amide lone pairs perpendicular to the equatorial plane. On the other hand, **12** lies closer to that in Figure 5c

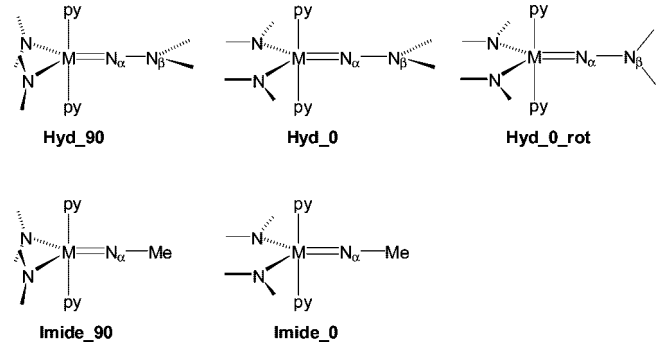

Figure 7. Simplified models based on $Ti(NR)(NMe_2)_2(py)_2$ (R = NMe_2, Me) used to evaluate the effect of changing the orientation or type of various substituents. The suffixes "90" and "0" refer to the magnitude of the torsion angles $N_\alpha-Ti-N_{am}-Me$ (cf. the torsion angles N(1)−Ti(1)−N(3,4)−Si or N(1)−Ti(1)−N(3,4)−C in Table 3).

(lone pairs lying in the equatorial plane), and on going from one to the other, the $Ti-N_{am}$ distances progressively shorten while both the $Ti=N_\alpha$ and $N_\alpha-N_\beta$ lengthen (Table 3). A clear understanding of these effects will be important for understanding the reactivity patterns of such compounds and will aid selection of suitable supporting ligands. Therefore, using a series of simplified models based on $Ti(NR)(NMe_2)_2(py)_2$ (R = NMe_2, Me; Figure 7), we investigated the differing π-donor effects of the various diamide-amide ligands in **2** and **10**−**12**. We varied the orientation of the β-NMe_2 group and compared the bonding between model hydrazide systems $(L)Ti{=}NNMe_2$ and the corresponding imides (L)Ti=NMe. The model compounds are shown in Figure 7 along with the abbreviations used. Table 4 lists key geometrical parameters and relative energies for the various systems.

The model systems (Figure 7; see the Computational Details for full details) were constrained to C_{2v} symmetry with planar β-nitrogens in the case of the hydrazides (in the real systems **2** and **10**−**12** the phenyl substituents stabilize the trigonal-planar N_β geometry). To understand the structural variations (Table 4) between the different models, we analyzed the electronic structures using the NBO (natural bond orbital) method.[91,92] The advantage of this approach is that it aids interpretation of the bonding in a transparent and intuitive way in terms of the closest

(91) Reed, A. E.; Curtiss, L. A.; Weinhold, F. *Chem. Rev.* **1988**, *88*, 899.

Table 4. Key Geometrical Parameters and Relative Energies (E_{rel}) for the Various Model Systems Ti(NR)(NMe$_2$)$_2$(py)$_2$ (R = NMe$_2$, Me) Studied[a]

parameter	Hyd_90	Hyd_0	Hyd_0_rot	Imide_90	Imide_0
Ti=N$_\alpha$ (Å)	1.734	1.729	1.719	1.705	1.708
N$_\alpha$−N$_\beta$ (Å)	1.331	1.341	1.355		
Ti−N$_{am}$ (Å)	2.048	1.975	1.980	2.050	1.970
Ti−py (Å)	2.288	2.306	2.317	2.269	2.307
N$_\alpha$−Ti−N$_{am}$ (deg)	114.4	114.2	110.6	114.2	113.7
N$_{am}$−Ti−N$_{am}$ (deg)	131.1	131.5	138.8	131.8	132.5
E_{rel} (kJ mol^{-1})	72.2	0.0	33.6	93.6	0.0

[a] The energies for **Hyd_90** and **Hyd_0_rot** are expressed relative to that of **Hyd_0**. The E_{rel} of **Imide_90** is expressed relative to that of **Imide_0**. N$_{am}$ refers to the NMe$_2$ amide nitrogens. See Figure 7 for the geometries.

idealized Lewis structure. For all of the models Ti(NR)(NMe$_2$)$_2$(py)$_2$ the NBO analysis found NLMOs (natural localized molecular orbitals) corresponding to Ti−N$_\alpha$ and Ti−N$_{am}$ σ bonds, two Ti−N$_\alpha$ π bonds (one for each of π_v and π_h), and a Ti−N$_{am}$ π bond to each NMe$_2$. For the hydrazide models a "lone pair" essentially localized (see below) on N$_\beta$ was also found. These NLMOs clearly correspond to the expected Lewis structures **18** and **19** for the hydrazido(2−) and imido models, respectively. The main % atomic contributions to these NLMOs are given in Table 5.

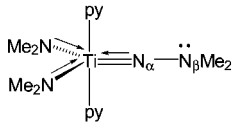

18

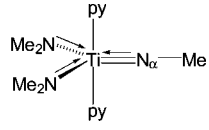

19

Orientation of Amide Lone Pairs. Going from model **Hyd_90** to **Hyd_0** rotates the NMe$_2$ lone pairs from lying in the equatorial plane to being perpendicular to it. This models the general trend on going from **2** to **12** in the real systems. For the model systems this results in a very slight shortening of Ti=N$_\alpha$, a significant shortening of Ti−N$_{am}$, and a lengthening of N$_\alpha$−N$_\beta$. There is an associated stabilization of 72.2 kJ mol^{-1}. The shorter Ti−N$_{am}$ may be attributed to the better match between the amide lone pairs and the 1b$_2$ and 1a$_2$ acceptor MOs of Ti (cf. Figure 4) than the 1a$_1$ and 1b$_1$ alternatives. Consistent with this, the NBO analysis (Table 5) shows an increased covalency in both the σ and π Ti−N$_{am}$ NLMOs.[93] The competition between the amide lone pairs and the hydrazide π_v for the Ti 1b$_2$ acceptor MO results in a diminished π_v(Ti−N$_\alpha$) interaction. Conversely, the corresponding π_h(Ti−N$_\alpha$) bonding is improved since the Ti 1b$_1$ no longer overlaps with the amide lone pairs. Importantly, the higher %Ti in σ(Ti−N$_\alpha$) shows that the NNMe$_2$ ligand is a better σ donor in **Hyd_0** because there is no longer destabilization of the Ti 1a$_1$ orbital (Ti−N$_\alpha$ σ* antibonding) through π donation from the amide a$_1$ lone pair. Thus there is a combination of σ and π effects that contribute to the stabilization of isomer **Hyd_0** compared with **Hyd_90**, and the variation in the Ti=N$_\alpha$ distance is a composite of increased σ(N$_\alpha$) and π_h donation and diminished π_v donation.

We have also calculated the NPA (natural population analysis) charges for the fragments {NR}, {(NMe$_2$)$_2$} and {Ti(py)$_2$} for the five model systems Ti(NR)(NMe$_2$)$_2$(py)$_2$ (see Table S4 of the Supporting Information). On going from **Hyd_90** to **Hyd_0**, the {Ti(py)$_2$} fragment charge decreases from +1.753*e* to +1.585*e* while the {(NMe$_2$)$_2$} charge changes from −1.173*e* to −1.000*e*. The {NNMe$_2$} charge on the other hand decreases by only 0.005*e*. Similar variations were found for the imido systems and again illustrates the effect of rotating the amide lone pairs on NMe$_2$→Ti electron donation.

Rotation of the N$_\beta$Me$_2$ Group. All of the experimental systems **2**−**12** have the hydrazide NPh$_2$ substituents lying in the equatorial plane. As discussed above, this should allow best overlap of the hydrazide π_v orbital with the lower energy acceptor orbital on Ti. To quantify this analysis, we examined the model **Hyd_0_rot** (Figure 7), which has the N$_\beta$Me$_2$ group rotated by 90°. This was accompanied by a destabilization (ΔE_{rel}) of 33.6 kJ mol^{-1} (Table 4) relative to **Hyd_0**, consistent with experimental observations. The NLMO analysis for **Hyd_0_rot** is similar to that for **Hyd_0** with regard to the Ti−N$_{am}$ interactions and Ti−N$_\alpha$ σ interactions. However, there is a significant effect on the Ti−N$_\alpha$ π interactions as expected. Whereas the π_v(Ti−N$_\alpha$) bond is significantly more covalent than π_h(Ti−N$_\alpha$) in **Hyd_0** (and also **Hyd_90**) for the reasons discussed above, in **Hyd_0_rot** the Ti−N$_\alpha$ π bonding is much more cylindrical. This is because the higher energy NNMe$_2$ π donor (π_v) now has to interact with a higher energy Ti d$_\pi$ acceptor (1b$_1$, which is also slightly Ti−N$_{am}$ σ* antibonding), while the π_h donor accesses the lower energy Ti 1b$_2$ orbital. Overall there is a net gain in negative charge of the {NNMe$_2$} and {(NMe$_2$)$_2$} fragments (Table S4 in the SI) and increase in positive charge for {Ti(py)$_2$}, showing that this orientation of the N$_\beta$Me$_2$ group results in a reduced net donation from both the diamide and hydrazide ligands, despite the slight shortening of the Ti−N$_\alpha$ bond length.

N$_\alpha$−N$_\beta$ Interaction. The weakening of the N$_\alpha$−N$_\beta$ bond is an important aspect of metal hydrazide chemistry from the point of view of its eventual cleavage. Several reports from group 4 have found facile cleavage of this bond, especially in π-loaded systems.[29,34,35] Experimentally (**2**−**12**) and computationally it is found that rotation of the amide lone pairs results in a slightly longer N$_\alpha$−N$_\beta$ distance ($\Delta \approx 0.01$ Å). Furthermore, the model **Hyd_0_rot** shows a further ca. 0.015 Å lengthening of N$_\alpha$−N$_\beta$ and shortening of Ti−N$_\alpha$. The NBO and NLMO analyses offer an explanation of these trends in Ti−N$_\alpha$ and N$_\alpha$−N$_\beta$ distances.

As mentioned, the NBO analyses of **Hyd_90**, **Hyd_0**, and **Hyd_0_rot** are consistent with the Lewis structure **18**, in which there is a formal "lone pair" mainly localized on N$_\beta$. This is confirmed by the NLMO analysis for this orbital (Table 5; %N ca. 87−89%). However, this also finds that the electron pair is partially delocalized into the *antibonding* π^*_v(Ti−N$_\alpha$) orbital, accounting for the nonzero %Ti and %N$_\alpha$ contributions to the "lone pair" NLMO (see Figure S2 of the Supporting Information). Clearly, this N$_\beta$→π^*_v(Ti−N$_\alpha$) interaction therefore simultaneously *weakens* the Ti−N$_\alpha$ bond and *strengthens* the N$_\alpha$−N$_\beta$ bond. The extent of the interaction will vary according to the properties (energy and %N$_\alpha$ character) of the π^*_v(Ti−N$_\alpha$) orbital. On going from **Hyd_90** to **Hyd_0**, the π^*_v(Ti−N$_\alpha$) orbital is destabilized due to competition with the amide lone pairs for the Ti 1b$_2$ acceptor orbital, and in **Hyd_0_rot** the NNMe$_2$ π_v donor has to use the higher energy 1b$_1$ orbital.

(92) Weinhold,F.; Landis, C. R. *Valency and Bonding: A Natural Bond Orbital Donor-Acceptor Perspective*; Cambridge University Press: Cambridge, 2005.

(93) Because of the higher electronegativity of nitrogen, all of the occupied NLMOs have a higher %N contribution than %Ti. Therefore an increased %Ti and decreased %N contribution for a given NLMO on going from one model to another is evidence of improved covalency in the orbital under consideration. From the perspective of fragment MO interactions this relates to a decreased energy separation and/or improved overlap between the participating orbitals.

Table 5. NLMO Analysis for the Various Model Systems Ti(NR)(NMe$_2$)$_2$(py)$_2$ (R = NMe$_2$, Me) Studied[a]

electron pair	Hyd_90	Hyd_0	Hyd_0_rot	Imide_90	Imide_0
σ(Ti−N$_\alpha$)	11.9% Ti	15.7% Ti	15.8% Ti	16.1% Ti	18.4% Ti
	86.2% N$_\alpha$	83.6% N$_\alpha$	83.0% N$_\alpha$	83.2% N$_\alpha$	81.2% N$_\alpha$
π_v(Ti−N$_\alpha$)	36.3% Ti	32.7% Ti	28.5% Ti	27.6% Ti	25.4% Ti
	62.1% N$_\alpha$	65.6% N$_\alpha$	69.5% N$_\alpha$	69.9% N$_\alpha$	72.0% N$_\alpha$
π_h(Ti−N$_\alpha$)	16.7% Ti	18.4% Ti	22.5% Ti	21.2% Ti	22.0% Ti
	80.7% N$_\alpha$	78.8% N$_\alpha$	75.3% N$_\alpha$	76.3% N$_\alpha$	75.2% N$_\alpha$
"lone pair" (N$_\beta$)	5.2% Ti	4.5% Ti	3.6% Ti		
	3.3% N$_\alpha$	2.5% N$_\alpha$	1.8% N$_\alpha$		
	86.7% N$_\beta$	88.3% N$_\beta$	89.0% N$_\beta$		
σ(Ti−N$_{am}$)	9.2% Ti	11.9% Ti	11.3% Ti	9.0% Ti	12.0% Ti
	87.9% N$_{am}$	85.6% N$_{am}$	86.1% N$_{am}$	87.3% N$_{am}$	85.4% N$_{am}$
π(Ti−N$_{am}$)	8.9% Ti	9.2% Ti	9.8% Ti	8.1% Ti	8.8% Ti
	85.2% N$_{am}$	83.6% N$_{am}$	83.1% N$_{am}$	85.7% N$_{am}$	83.4% N$_{am}$

[a] The % contributions are for the stated atoms in the respective NLMOs. See Figure 7 for the geometries. NPA (natural population analysis) charges for the {Ti(py)$_2$}, {NR}, and {(NMe$_2$)$_2$} fragments are given in Table S4 of the Supporting Information.

Table 6. X-ray Data Collection and Processing Parameters for Ti(NNPh$_2$)Cl$_2$(py)$_3$ (7), Ti(NNPh$_2$)Cl$_2$(py′)$_3$ (8), Ti(NNPh$_2$)(N$_2$N^{C_2,Me})(py) (2), Ti(NNPh$_2$)(N$_2$N^{C_2,SiMe_3})(py) (10), Ti(NNPh$_2$)(N$_2$N^{C_3,Me})(py) (11), and Ti(NNPh$_2$)(N$_2$N^{py})(py) (12)

	7	8	2	10	11	12
empirical formula	$C_{27}H_{25}Cl_2N_5Ti$	$C_{39}H_{49}Cl_2Ti$	$C_{28}H_{44}N_6Si_2Ti$	$C_{30}H_{50}N_6Si_3Ti$	$C_{30}H_{48}N_6Si_2Ti$	$C_{32}H_{44}N_6Si_2Ti$
fw	538.33	706.66	568.77	626.93	596.82	616.81
temp/K	150	150	150	150	150	150
wavelength/Å	0.71073	0.71073	0.71073	0.71073	0.71073	0.71073
space group	*C*2/*c*	*P*2$_1$/*c*	*P*$_1$	$P\bar{1}$	*P* 2$_1$/*c*	$P\bar{1}$
a/Å	14.0110(4)	22.2899(2)	10.1794(5)	10.3113(2)	11.5182(2)	10.1894(2)
b/Å	19.8007(6)	17.6264(2)	11.1800(7)	11.9118(3)	14.5639(3)	10.3302(2)
c/Å	9.4425(3)	19.8028(2)	13.8952(8)	14.0949(3)	20.0751(4)	17.9754(4)
α/deg	90	90	89.726(3)	92.1330(10)	90	95.5849(10)
β/deg	93.9572(12)	91.9807(6)	77.178(2)	90.7564(10)	100.6813(8)	103.2464(11)
γ/deg	90	90	85.912(3)	90.6550(10)	90	111.5826(10)
V/Å^3	2613.36(14)	7775.69(14)	1537.9(2)	1729.75(7)	3309.25(11)	1677.77(6)
Z	4	8	2	2	4	2
d(calcd)/Mg·m^{-3}	1.368	1.207	1.228	1.204	1.198	1.221
abs coeff/mm^{-1}	0.557	0.390	0.383	0.380	0.359	0.357
R indices: R_1 =	0.0337	0.0397	0.0728	0.0350	0.0429	0.0524
[$I > 3\sigma(I)$]:[a] R_w =	0.0367	0.0474	0.0800	0.0369	0.0387	0.0448

[a] $R_1 = \sum||F_o| - |F_c||/\sum|F_o|$; $R_w = \sqrt{\{\sum w(|F_o| - |F_c|)^2/\sum w|F_o|^2\}}$.

Therefore the N$_\beta$→π^*_v(Ti−N$_\alpha$) interaction is diminished along this distortion coordinate, consistent with the computed bond length trends. Indeed, the second-order perturbation energy associated with the N$_\beta$→π^*_v(Ti−N$_\alpha$) interaction decreases from **Hyd_90** to **Hyd_0** and finally to **Hyd_0_rot** (141.9, 124.1, and 103.4 kJ mol^{-1}, respectively) due to both a larger energy gap (0.26, 0.27, and 0.28 au, respectively) and a smaller Fock matrix element $F(i,j)$ (0.086, 0.080, and 0.074 au, respectively). This further explains the trends in the composition of the lone pair on N$_\beta$ in Table 5.

Comparison with Imido Systems. The NLMO analysis for the imido systems **Imide_90** and **Imide_0** reveals analogous trends, and in fact the latter is 93.6 kJ mol^{-1} more stable. The Ti−N$_{am}$ distances shorten significantly (Δ(Ti−N$_{am}$) = −0.08 Å), whereas (as for the hydrazido compounds) no significant change is registered for Ti−N$_\alpha$. These small changes in Ti−N$_\alpha$ for the hydrazido and imido systems show there is no significant net electronic driving force for Ti−N$_\alpha$ bond length change, despite varying the supporting diamide ligand set. Examination of the π_v(Ti−N$_\alpha$) and π_h(Ti−N$_\alpha$) NLMOs shows a much more cylindrical π-bonding manifold than is found in the corresponding hydrazide systems. As expected, the π_h(Ti−N$_\alpha$) NLMO is more based on N$_\alpha$ owing to the higher energy of the Ti 1b$_1$ acceptor MO.

The Ti−N$_\alpha$ bond distances in **Imide_90** and **Imide_0** are ca. 0.020−0.030 Å shorter than the corresponding values for **Hyd_90** and **Hyd_0**. This is consistent with the differences found in the real systems Ti("N$_2$N")(NR)(py) ("N$_2$N" = N$_2$N^{C_2,SiMe_3} or N$_2$N^{py}; R = ^{t}Bu or NNPh$_2$; Δ(Ti−N$_\alpha$) = 0.032(4)−0.035(3) Å).[69,81] One Ti−N$_\alpha$ bond-lengthening effect is due to the N$_\beta$→π^*_v(Ti−N$_\alpha$) interaction noted above. A second contribution is the reduced σ-donor ability of NNR$_2$ compared to NR because of the increased electron-withdrawing inductive effect of N$_\beta$R$_2$ compared to alkyl. This is evident in the %Ti,N contributions for the σ(Ti−N$_\alpha$) NLMOs in the two types of model system. The NLMOs for the hydrazido models are more localized on N$_\alpha$ in each case compared to the imido analogues. A similar conclusion with regard to σ-donor abilities was reached previously (based on fragment MO Mulliken population analyses) in comparing the Ti−N$_\alpha$ bonding in the model complexes Ti(NMe){HC(pz)$_3$}Cl$_2$ and Ti(NMe){HC(pz)$_3$}Cl$_2$.[31]

Comparison of Model and Experimental Systems. The shortening of the av Ti−N$_{am}$ distances from 2.028 to 1.974 Å from **2** to **12** (Table 3) is reproduced well by the models **Hyd_90** (Ti−N$_{am}$ = 2.048 Å) and **Hyd_0** (Ti−N$_{am}$ = 1.975 Å). The increase in the N$_\alpha$−N$_\beta$ distance is also well reproduced (0.01 Å in both experiment and theory). However, on going from **2** to **12** in the experimental systems, the Ti−N$_\alpha$ distance lengthens from 1.733(5) to 1.759(2) Å, whereas in the model systems there is a very small decrease from 1.734 to 1.729 Å. This apparent discrepancy can be attributed to significant steric interactions between the hydrazide phenyl substituents and the equatorial NSiMe$_3$ groups, as the latter move up into the equatorial plane and become more oriented toward the NNPh$_2$. This effect is probably the origin of the relatively large jump of ca. 0.02 Å in Ti−N$_\alpha$ bond length between Ti(NNPh$_2$)(N$_2$N^{C_2,Me})(py) (**2**) and Ti(NNPh$_2$)(N$_2$N^{C_2,SiMe_3})(py) (**10**) as the diamide-amine

N-Me group is replaced by $SiMe_3$. Thus a balance of real system steric factors and underlying electronic factors leads to the observed structural trends and (most likely) controls the reactivity patterns.

Conclusions

Far from being simple "imido analogues", terminal group 4 hydrazides can exhibit novel and potentially catalytic reactivity of the M═N−NR_2 functional group.[29,34,35,94,95] In this contribution, based on new readily available synthons, we have reported a comprehensive study of the synthesis and bonding of a new family of titanium diphenyl hydrazides using the important diamide-amine class of supporting ligands, among others. Through this series, the ligand coordination number, steric requirements, chelate ring size, and amide π-donor ability may be controlled. Detailed structural and computational studies of a series of closely related model complexes have defined the parameters, both steric and electronic, which influence the energies of these systems and the Ti−N_{am}, N_α−N_β, and Ti−N_α distances. Depending on their relative orientations, competition between the amide and hydrazide nitrogen $2p_\pi$ lone pairs modifies the π_v(Ti−N_α) NLMOs, which in turn leads to poorer N_α−N_β π bonding and a less stabilized β-nitrogen. The weakening of the N_α−N_β bond through N_{am}→Ti π donation to the relevant d_π AO echoes the dramatic weakening that occurs in the Schrock and Chatt catalytic cycles on addition of an external electron, just prior to proton-induced cleavage.

Ligands that deploy steric bulk in the vicinity of the Ti═$NNPh_2$ functional group can also lead to lengthened Ti−N_α bonds. Our synthetic and computational results also shed light on the high reactivity so far found for the terminal zirconium hydrazides $Cp_2Zr(NNPh_2)(DMAP)$[29] and $Zr(N_2N^{py*})(NNPh_2)(py)$, which have reactive N_α−N_β bonds that undergo unique insertion reactions.[35] In these systems we again expect the inherent "π-loaded" nature[96] to result in destabilized π_v(Zr−N_α) NLMOs just as for the diamide-amine-supported titanium systems described above. Furthermore, the less stabilized $4d_\pi$ AO of Zr is also expected to lead to poorer N_β→π^*_v(Zr−N_α) interactions. Indeed, the N_α−N_β bond distance of 1.398(3) Å in $Zr(N_2N^{py*})(NNPh_2)(py)$, which also features bulky $SiMe_2{}^tBu$ substituents, is the longest known for a terminal diphenyl hydrazide.

Finally we recall that terminal metal hydrazides are commonly first-formed products in the functionalization of molecular dinitrogen.[7−12] Incorporating some of these above-mentioned design principles into transition metal compounds suitable for N_2 activation may lead ultimately to new dinitrogen functionalization processes via activated terminal hydrazides.

Experimental Section

General Methods and Instrumentation. All manipulations were carried out under an inert atmosphere of argon or dinitrogen using standard Schlenk-line or drybox procedures. Solvents were predried over activated 4 Å molecular sieves and refluxed over sodium (toluene), sodium/potassium (pentane, diethyl ether), potassium (tetrahydrofuran), or calcium hydride (dichloromethane) under a dinitrogen atmosphere and collected by distillation. Alternatively, solvents were degassed by sparging with dinitrogen and dried by passing through a column of activated alumina. Deuterated solvents were dried over potassium (C_6D_6) or P_2O_5 (CD_2Cl_2), distilled under reduced pressure, and stored under dinitrogen in Young's Teflon valve ampules.

Solution NMR samples were prepared under a dinitrogen atmosphere in a drybox, in 5 mm Wilmad NMR tubes possessing Young's Teflon valves. ^1H and ^{13}C NMR spectra were recorded on a Varian Mercury 300 spectrometer at ambient temperature. All spectra were internally referenced to either residual protio-solvent (^1H) or solvent (^{13}C) resonances and are reported relative to tetramethylsilane (δ = 0 ppm). Chemical shifts are quoted in δ (ppm) and coupling constants in Hz. Where necessary, ^1H and ^{13}C assignments were assisted by the use of two-dimensional ^1H−^1H and ^1H−^{13}C correlation experiments. IR spectra were recorded on a Perkin-Elmer 1710 FTIR spectrometer. Samples were prepared in a drybox as Nujol mulls between NaCl plates. IR data are quoted as wavenumbers (cm^{-1}) within the range 4000−400 cm^{-1}. Mass spectra were recorded by the departmental service, and elemental analyses were carried out by the Elemental Analysis Service at the London Metropolitan University.

Starting Materials. The compounds $Ti(N^tBu)Cl_2(py)_3$,[66] $[Ti(NNMe_2)Cl_2(py)_2]_2$,[31] $Li_2N_2N^{C_3,Me}$,[97] $Li_2N_2N^{C_2,SiMe_3}$,[98] $Li_2N_2N^{C_3,Me}$,[97] $Li_2N_2N^{py}$,[99] Li_2N_2NN',[78] Li_2Me_4taa,[100] and $Na_2O_2NN'\cdot 0.16(THF)$[101] were prepared according to the literature methods. $Ti(N^tBu)Cl_2(py')_3$ was prepared by analogy with the literature methods for $Ti(N^tBu)Cl_2(py)_3$ and $Ti(N^tBu)Cl_2(py')_2$.[66,74] Diphenylhydrazine was obtained from Sigma-Aldrich as the hydrogen chloride salt, from which the free hydrazine was obtained by basification, drying, and removal of residual solvent, followed by distillation under inert atmospheric conditions. Pyridine was dried over freshly ground CaH_2 and distilled before use. Other reagents were obtained commercially and used as received.

$Ti(NNPh_2)Cl_2(py)_3$ (7). To a stirred solution of $Ti(N^tBu)Cl_2(py)_3$ (5.00 g, 11.7 mmol) in benzene (50 mL) was added H_2NNPh_2 (2.15 g, 11.7 mmol) in benzene (10 mL) dropwise over 15 min. The orange solution was stirred for 14 h, resulting in a dark brown solution and a yellow precipitate. The solution was filtered, and the precipitate washed with pentane (3 × 20 mL) and filtered. The yellow solid product was dried *in vacuo*. Yield: 5.60 g (89%). Diffraction-quality crystals were grown from a saturated benzene solution.

^1H NMR (CD_2Cl_2, 299.9 MHz, 293 K): δ 9.01 (4 H, d, ^3J = 5 Hz, *o*-H of *cis*-NC_5H_4), 8.59 (2 H, br m, coupling not resolved, *o*-H of *trans*-NC_5H_4), 7.86 (2 H, t, ^3J = 7.7 Hz, *p*-H of *cis*-NC_5H_4), 7.68 (1 H, br m, coupling not resolved *p*-H of *trans*-NC_5H_4), 7.41 (4 H, d, ^3J = 7.3 Hz, *o*-C_6H_5), 7.29−7.13 (10 H, overlapping peaks, *m*-C_6H_5, *m*-H of *cis*- and *trans*-NC_5H_4), 6.99 (2 H, t, ^3J = 7.3 Hz, *p*-C_6H_5). IR (NaCl plates, Nujol mull, cm^{-1}): ν 1653 (w), 1604 (s), 1594 (s), 1586 (s), 1559 (w), 1543 (m), 1487 (m), 1447 (s), 1337 (w), 1313 (w), 1269 (s), 1219 (m), 1168 (w), 1154 (w), 1108 (w), 1070 (m), 1043 (m), 1028 (w), 1013 (m), 842 (w), 753 (m), 693 (s), 636 (w). Anal. Found (calcd for $C_{27}H_{25}Cl_2N_5Ti$): C, 60.0 (60.2); H, 4.8 (4.7); N, 12.9 (13.0). A ^{13}C NMR spectrum could not be obtained due to the low solubility of **7** in suitable solvents.

Alternative Synthesis of $[Ti(NNPh_2)Cl_2(py)_2]_2$ (4). $Ti(NNPh_2)Cl_2(py)_3$ (**7**, 0.50 g, 0.93 mmol) was held under a dynamic vacuum (4 × 10^{-2} mbar) for 14 h, then washed with pentane (2 × 25 mL) to quantitatively yield $[Ti(NNPh_2)Cl_2(py)_2]_2$

(94) Herrmann, H.; Wadepohl, H.; Gade, L. H. *Dalton Trans.* **2008**, 2111.
(95) Mindiola, D. J. *Angew. Chem., Int. Ed.* **2008**, *47*, 1557.
(96) Green, J. C. *Chem. Soc. Rev.* **1998**, *27*, 263.
(97) Ward, B. D.; Dubberley, S. R.; Maisse-Francois, A.; Gade, L. H.; Mountford, P. *Dalton Trans.* **2002**, 4649.
(98) Cloke, F. G. N.; Hitchcock, P. B.; Love, J. B. *J. Chem. Soc., Dalton Trans.* **1995**, 25.
(99) Galka, C. H.; Trösch, D. J. M.; Schubart, M.; Gade, L. H.; Radojevic, S.; Scowen, I. J.; McPartlin, M. *Eur. J. Inorg. Chem.* **2000**, 2577.
(100) Black, D. G.; Swenson, D. C.; Jordan, R. F.; Rogers, R. D. *Organometallics* **1995**, *14*, 3539.
(101) Toupance, T.; Dubberley, S. R.; Rees, N. H.; Tyrrell, B. R.; Mountford, P. *Organometallics* **2002**, *21*, 1367.

(**4**) as a yellow-green solid. The NMR data for **4** were consistent with those previously reported.[31]

Ti(NNPh$_2$)Cl$_2$(py′)$_3$ (8). To a stirred solution of Ti(N^{t}Bu)Cl$_2$(py′)$_3$ (2.00 g, 3.37 mmol) in benzene (50 mL) was added H_2NNPh_2 (0.62 g, 3.37 mmol) in benzene (10 mL) dropwise over 15 min. The orange solution was stirred for 14 h, resulting in a dark brown solution. Volatiles were removed under reduced pressure, and the dark brown solid was washed with pentane (3 × 20 mL) and filtered. The yellow solid product was dried *in vacuo*. Yield: 1.75 g (74%). Diffraction-quality crystals were grown from a saturated pentane solution.

^{1}H NMR (C_6D_6, 299.9 MHz, 293 K): δ 9.34 (4 H, d, ^3J = 6.5 Hz, *o*-H of *cis*-NC_5H_4), 9.03 (2 H, d, ^3J = 4.7 Hz, *o*-H of *trans*-NC_5H_4), 8.19 (4 H, d, ^3J = 7.7 Hz, *o*-C_6H_5), 7.29 (4 H, dd, ^3J = 7.7 and 7.0 Hz, *m*-C_6H_5), 6.88 (2 H, t, ^3J = 7.0 Hz, *p*-C_6H_5), 6.65 (2 H, d, ^3J = 4.7 Hz, *m*-H of *trans*-NC_5H_4), 6.60 (4 H, d, ^3J = 6.5 Hz, *m*-H of *cis*-NC_5H_4), 0.90 (9 H, s, *trans*-CMe_3), 0.81 (18 H, s, *cis*-CMe_3). ^{13}C{^{1}H} NMR (C_6D_6, 75.4 MHz, 293 K): δ 162.2 (*p*-C of *cis*-NC_5H_4), 160.1 (*p*-C of *trans*-NC_5H_4), 152.9 (*o*-C of *cis*-NC_5H_4), 152.2 (*o*-C of *trans*-NC_5H_4), 145.8 (*i*-C_6H_5), 129.4 (*m*-C_6H_5),123.3 (*p*-C_6H_5), 121.2 (*m*-C of *cis*-NC_5H_4), 120.6 (*m*-C of *trans*-NC_5H_4), 120.0 (*o*-C_6H_5), 34.9 (*cis*-$\underline{C}Me_3$), 34.7 (*trans*-$\underline{C}Me_3$), 30.5 (*trans*-CMe_3), 30.3 (*cis*-CMe_3). IR (NaCl plates, Nujol mull, cm^{-1}): ν 1613 (s), 1585 (s), 1543.7 (s), 1461 (s), 1418 (m), 1368 (m), 1314 (s), 1274 (s), 1230 (s), 1201 (m), 1184 (w), 1172 (w), 1070 (s), 1022 (m), 995 (w), 843 (s), 803 (s), 750 (s), 725 (s) 695 (m), 637 (w), 572 (w). Anal. Found (calcd for $C_{39}H_{49}Cl_2N_5Ti$): C, 66.4 (66.3); H, 7.1 (7.0); N, 9.8 (9.9).

Ti(NNPh$_2$)(N$_2$N^{C_2,Me})(py) (2). To a stirred mixture of Ti(NNPh$_2$)Cl$_2$(py)$_3$ (2.00 g, 3.72 mmol) and $Li_2N_2N^{C_2,Me}$ (1.01 g, 3.72 mmol) was added toluene (60 mL), all at −78 °C. The green suspension was allowed to warm to room temperature and stirred for a further hour, resulting in a dark brown solution. Volatiles were removed under reduced pressure, and the dark oily solid was extracted into Et_2O (3 × 30 mL) and filtered twice. Volatiles were removed under reduced pressure to yield a brown solid, which was washed with pentane (3 × 5 mL) cooled to −78 °C. The green solid product was dried *in vacuo*. Yield: 1.37 g (65%). Diffraction-quality crystals were grown from a saturated pentane solution at −30 °C.

^{1}H NMR (C_6D_6, 299.9 MHz, 293 K): δ 8.68 (2 H, d, ^3J = 6.4 Hz, *o*-NC_5H_5), 7.87 (4 H, d, ^3J = 7.6 Hz, *o*-C_6H_5), 7.31 (4 H, app. t, app. ^3J = 7.1 and 7.6 Hz, *m*-C_6H_5), 6.91 (2 H, t, ^3J = 7.1 Hz, *p*-C_6H_5), 6.68 (1 H, t, ^3J = 7.6 Hz, *p*-NC_5H_5), 6.38 (2 H, app. t, app. ^3J = 6.4 and 7.6 Hz, *m*-NC_5H_5), 3.56, 3.39 (2 × 2 H, 2 × m, $C\underline{H}_2NSiMe_3$), 2.74, 2.56 (2 × 2 H, 2 × m, $C\underline{H}_2NMe$), 2.62 (3 H, s, NMe), 0.03 (18 H, s, $SiMe_3$). ^{13}C{^{1}H} NMR (C_6D_6, 75.4 MHz, 293 K): δ 153.9 (*o*-NC_5H_5), 147.9 (*i*-C_6H_5), 138.7 (*p*-NC_5H_5), 129.3 (*m*-C_6H_5), 124.0 (*m*-NC_5H_5), 122.2 (*p*-C_6H_5), 119.1 (*o*-C_6H_5), 63.6 ($\underline{C}H_2NMe$), 50.7 (NMe), 48.2 ($\underline{C}H_2NSiMe_3$), 1.9 ($SiMe_3$). IR (NaCl plates, Nujol mull, cm^{-1}): ν 1600 (m), 1586 (s), 1486 (s), 1445 (s), 1308 (w), 1298 (w), 1240 (s), 1211 (w), 1168 (w), 1078 (m), 1064 (m), 1041 (m), 1012 (w), 989 (w), 919 (s), 841 (s), 799 (m), 745 (s), 697 (s), 636 (w), 621 (w). EI-MS: *m*/*z* 489 (16%) [M − py]$^+$, 168 (73%) [NPh$_2$]$^+$. Anal. Found (calcd for $C_{28}H_{44}N_6Si_2Ti$): C, 59.0 (59.1); H, 7.7 (7.8); N, 14.7 (14.8).

Ti(NNPh$_2$)(N$_2$N^{C_2,SiMe_3})(py) (10). To a stirred mixture of [Ti(NNPh$_2$)Cl$_2$(py)$_2$]$_2$ (1.00 g, 2.18 mmol) and $Li_2N_2N^{C_2,SiMe_3}$ (0.72 g, 2.18 mmol) was added toluene (60 mL), all at −78 °C. The green suspension was allowed to warm to room temperature and stirred for a further 90 min, resulting in a dark brown solution. Volatiles were removed under reduced pressure, and the dark oily solid was extracted into Et_2O (2 × 30 mL) and filtered. Volatiles were removed under reduced pressure to yield a brown solid, which was washed with pentane (3 × 5 mL) cooled to −78 °C. The green solid product was dried *in vacuo*. Yield: 0.36 g (26%). Diffraction-quality crystals were grown from a saturated pentane solution at −30 °C.

^{1}H NMR (C_6D_6, 299.9 MHz, 293 K): δ 8.66 (2 H, d, ^3J = 6.4 Hz, *o*-NC_5H_5), 7.78 (4 H, d, ^3J = 8.3 Hz, *o*-C_6H_5), 7.28 (4 H, app. t, app. ^3J = 7.1 and 8.3 Hz, *m*-C_6H_5), 6.89 (2 H, t, ^3J = 7.1 Hz, *p*-C_6H_5), 6.72 (1 H, t, ^3J = 7.6 Hz, *p*-NC_5H_5), 6.38 (2 H, app. t, app. ^3J = 6.4 and 7.6 Hz, *m*-NC_5H_5), 3.76 (2 H, m, $C\underline{H}_2NSiMe_3$ inner protons *cis* to py), 3.21 (2 H, m, $C\underline{H}_2NSiMe_3$ outer protons *cis* to py), 3.06 (2 H, m, $C\underline{H}_2NSiMe_3$ inner protons *trans* to py), 2.46 (2 H, m, $C\underline{H}_2NSiMe_3$ outer protons *trans* to py), 0.22 (9 H, s, $SiMe_3$ *trans* to py), 0.03 (18 H, s, $SiMe_3$ *cis* to py). ^{13}C{^{1}H} NMR (C_6D_6, 75.4 MHz, 293 K): δ 152.5 (*o*-NC_5H_5), 147.7 (*i*-C_6H_5), 138.4 (*p*-NC_5H_5), 129.2 (*m*-C_6H_5), 123.9 (*m*-NC_5H_5), 122.4 (*p*-C_6H_5), 119.9 (*o*-C_6H_5), 59.5 ($\underline{C}H_2NSiMe_3$ *trans* to py), 48.7 ($\underline{C}H_2SiMe_3$ *cis* to py), 1.8 ($SiMe_3$ *cis* to py), 0.6 ($SiMe_3$ *trans* to py). IR (NaCl plates, Nujol mull, cm^{-1}): ν 1600 (m), 1583 (m), 1489 (m), 1444 (s), 1345 (w), 1306 (w), 1295 (w), 1276 (m), 1256 (m), 1245 (m), 1211 (w), 1167 (w), 1067 (m), 1041 (w), 1024 (m), 1012 (w), 993 (w), 939 (s), 908 (w), 872 (m), 840 (s), 797 (w), 779 (m), 754 (w), 745 (m), 696 (m), 678 (w), 635 (w), 624 (w). EI-MS: *m*/*z* 168 (98%) [NPh$_2$]$^+$, 77 (77%) [C$_6$H$_6$]$^+$. Anal. Found (calcd for $C_{30}H_{50}N_6Si_3Ti$): C, 57.4 (57.5); H, 7.9 (8.0); N, 13.4 (13.4).

Ti(NNPh$_2$)(N$_2$N^{C_3,Me})(py) (11). To a stirred mixture of [Ti(NNPh$_2$)Cl$_2$(py)$_2$]$_2$ (1.00 g, 2.18 mmol) and $Li_2N_2N^{C_3,Me}$ (0.657 g, 2.18 mmol) was added toluene (60 mL), all at −78 °C. The green suspension was allowed to warm to room temperature and stirred for a further hour, resulting in a dark brown solution. Volatiles were removed under reduced pressure, and the dark oily solid was extracted into Et_2O (2 × 30 mL) and filtered. Volatiles were removed under reduced pressure to yield a brown solid, which was washed with hexane (3 × 5 mL) cooled to −78 °C. The brown solid product was dried *in vacuo*. Yield: 0.53 g (41%). Diffraction-quality crystals were grown from a saturated hexane solution at −30 °C.

^{1}H NMR (C_6D_6, 299.9 MHz, 293 K): δ 8.66 (2 H, d, ^3J = 6.4 Hz, *o*-NC_5H_5), 7.67 (4 H, d, ^3J = 7.6 Hz, *o*-C_6H_5), 7.25 (4 H, app. t, app. ^3J =7.6 and 7.8 Hz, *m*-C_6H_5), 6.90 (3 H, m, *p*-C_6H_5 and *p*-NC_5H_5), 6.61 (2 H, app. t, app. ^3J = 6.4 and 7.6 Hz, *m*-NC_5H_5), 3.93 (2 H, m, $C\underline{H}_2NSiMe_3$ inner protons), 3.28 (2 H, m, $C\underline{H}_2NSiMe_3$ outer protons), 2.55 (3 H, s, NMe), 2.23 (2 H, m, $C\underline{H}_2NMe$ inner protons), 1.99, (2 H, m, $C\underline{H}_2NMe$ outer protons), 1.33 (4 H, m, 2 × CH_2), 0.23 (18 H, s, $SiMe_3$). ^{13}C{^{1}H} NMR (C_6D_6, 75.4 MHz, 293 K): δ 151.8 (*o*-NC_5H_5), 147.6 (*i*-C_6H_5), 136.6 (*p*-NC_5H_5), 129.3 (*m*-C_6H_5), 123.7 (*m*-NC_5H_5), 122.3 (*p*-C_6H_5), 119.3 (*o*-C_6H_5), 60.6 ($\underline{C}H_2NMe$), 50.7 (NMe), 46.5 ($\underline{C}H_2NSiMe_3$), 30.8 (CH_2), 2.5 ($SiMe_3$). IR (NaCl plates, Nujol mull, cm^{-1}): ν 1596 (m), 1585 (m), 1488 (s), 1457 (s), 1442 (m), 1297 (m), 1255 (m), 1245 (s), 1209 (w), 1158 (w), 1146 (w), 1135 (m), 1078 (m), 1061 (m), 1036 (m), 1013 (m), 991 (w), 961 (w), 947 (m), 920 (w), 888 (m), 879 (m), 854 (s), 828 (s), 797 (m), 776 (m), 756 (m), 745 (s), 695 (s), 662 (w), 625 (m), 614 (m). EI-MS: *m*/*z* 517 (11%) [M − py]$^+$, 168 (100%) [NPh$_2$]$^+$. Anal. Found (calcd for $C_{30}H_{48}N_6Si_2Ti$): C, 60.4 (60.4); H, 8.2 (8.1); N, 13.9 (14.1).

Ti(NNPh$_2$)(N$_2$N^{py})(py) (12). To a stirred slurry of Ti(NNPh$_2$)Cl$_2$(py)$_3$ (1.67 g, 3.10 mmol) in toluene (50 mL), cooled to −78 °C, was added $Li_2N_2N^{py}$ (1.00 g, 3.10 mmol) in toluene (10 mL) dropwise over 15 min. The green-yellow slurry was allowed to warm to room temperature and stirred for 14 h, resulting in a dark brown solution. Volatiles were removed under reduced pressure, and the dark brown solid was extracted into Et_2O (3 × 30 mL) and filtered. Volatiles were removed under reduced pressure to yield a brown solid, which was stirred with pentane (2 × 50 mL) and filtered. The dark green solid product was dried *in vacuo*. Yield: 1.40 g (73%). Diffraction-quality crystals were grown from slow evaporation of a diethyl ether solution.

^{1}H NMR (C_6D_6, 299.9 MHz, 293 K): δ 9.44 (1H, d, py-H^6, ^3J = 4.1 Hz), 9.00 (2H, d, *o*-NC_5H_4, ^3J = 4.1 Hz), 7.82 (4 H, d, ^3J = 7.6 Hz, *o*-C_6H_5), 7.29 (4 H, app. t, app. ^3J =7.6 and 8.3 Hz,

m-C_6H_5), 7.03 (1 H, ddd, py-H^4, ^3J = 7.6 Hz, ^4J = 1.8 Hz) 6.93−6.85 (4 H, overlapping m, *p*-C_6H_5, *p*-NC_5H_4, and py-H^3), 6.61 (2 H, app t, *m*-NC_5H_4, app. ^3J = 6.8 Hz), 6.41 (1 H, dd, py-H^5, ^3J = 7.6 Hz, ^4J = 1.2 Hz), 3.79 (2 H, d, CHHNSi$_3$, ^2J = 12.3 Hz), 3.37 (2 H, d, CHHNSi$_3$, ^2J = 12.3 Hz), 1.20 (3 H, s, Me), −0.03 (18 H, s, NSiMe$_3$). $^{13}C\{^1H\}$ NMR (C_6D_6, 75.4 MHz, 293 K): δ 161.7(py-C^2), 152.4 (*o*-NC_5H_4), 151.9 (py-C^6), 148.1 (*i*-C_6H_5), 138.3 (py-C^4), 137.6 (*p*-NC_6H_5) 129.6 (*m*-C_6H_5), 123.8 (*m*-NC_5H_4), 122.2 (*p*-C_6H_5), 121.3 (py-C^5), 119.7 (py-C^3), 119.5 (*o*-C_6H_5), 64.3 ($\underline{C}H_2NSi_3$), 47.3(Me$\underline{C}$), 24.6 ($\underline{Me}C$), 1.3 (NSiMe$_3$). IR (NaCl plates, Nujol mull, cm^{-1}): ν 1596 (s), 1585 (s), 1559 (w), 1506 (s), 1486 (s), 1467 (m), 1313 (s), 1299 (m), 1282 (s), 1240 (s), 1212 (m), 1159 (w), 1134 (w), 1085 (s), 1063 (s) 1038 (s), 1023 (m), 1011 (w), 997 (w), 989 (w), 897 (s), 880 (s), 831 (w), 782 (w), 754 (s), 738 (m), 695 (m), 673 (w), 618 (w), 589 (w). EI-MS: *m*/*z* 168 (90%) $[NPh_2]^+$. Anal. Found (calcd for $C_{32}H_{44}N_6Si_2Ti$): C, 62.2 (62.3); H, 7.2 (7.2); N, 13.7 (13.6).

Ti(NNPh$_2$)(N$_2$NN′)(py) (13). To a stirred mixture of $[Ti(NNPh_2)Cl_2(py)_2]_2$ (0.30 g, 0.66 mmol) and Li_2N_2NN' (0.23 g, 0.66 mmol) was added toluene (30 mL), all at −78 °C. The yellow-green suspension was allowed to warm to room temperature and stirred for a further 90 min, resulting in a dark brown solution. Volatiles were removed under reduced pressure, and the brown solid was extracted into Et_2O (2 × 5 mL) and filtered. Volatiles were removed under reduced pressure to yield a green-brown solid, which was washed with pentane (3 × 5 mL) cooled to −78 °C. The dark green solid product was dried *in vacuo*. Yield: 0.12 g (31%).

^{1}H NMR (C_6D_6, 299.9 MHz, 293 K): δ 8.98 (1 H, d, ^3J = 6.5 Hz, 6-NC_5H_4), 7.75 (4 H, d, ^3J = 8.3 Hz, *o*-C_6H_5), 7.24 (4 H, app. t, app. ^3J = 8.3 and 7.6 Hz, *m*-C_6H_5), 6.87 (2 H, t, ^3J = 7.6 Hz, *p*-C_6H_5), 6.61 (1 H, app. t, app. ^3J = 7.6 and 7.7 Hz, 4-NC_5H_4), 6.12 (1 H, app. t, app. ^3J = 7.7 Hz, 5-NC_5H_4), 6.06 (1 H, d, ^3J = 7.6 Hz, 3-NC_5H_4), 3.66 (2 H, m, $\underline{H}_2NSiMe_3$ inner protons), 3.46 (2 H, m, $\underline{H}_2NSiMe_3$ outer protons), 3.01 (2 H, s, $\underline{H}_2NC_5H_4$), 2.60 (2 H, m, $\underline{H}_2N$ inner protons), 2.08 (2 H, m, $\underline{H}_2N$ outer protons), 0.45 (18 H, s, SiMe$_3$). $^{13}C\{^1H\}$ NMR (C_6D_6, 75.4 MHz, 293 K): δ 159.3 (2-NC_5H_5), 154.5 (6-NC_5H_5), 147.8 (*i*-C_6H_5), 140.0 (4-NC_5H_5), 129.5 (*m*-C_6H_5), 127.8, 123.5 (3-NC_5H_5 and 5-NC_5H_5), 122.0 (*p*-C_6H_5), 120.5 (o-C_6H_5), 57.3 ($\underline{C}H_2NC_5H_5$), 56.4 (NCH_2), 49.2 ($\underline{C}H_2NSiMe_3$), 3.2 (SiMe$_3$). IR (NaCl plates, Nujol mull, cm^{-1}): ν 1593 (m), 1583 (m), 1487 (s), 1312 (w), 1237 (m), 1168 (w), 1156 (w), 1086 (s), 1024 (m), 946 (m), 934 (m), 866 (m), 833 (s), 793 (m), 756 (w), 740 (m), 701 (w), 692 (w), 630 (w), 584 (w). EI-MS: *m*/*z* 168 (88%) $[NPh_2]^+$, 73 (88%) $[SiMe_3]$. Anal. Found (calcd for $C_{28}H_{42}N_6Si_2Ti$): C, 59.2 (59.3); H, 7.4 (7.5); N, 14.7 (14.8).

Alternative Synthesis of Ti(NNPh$_2$)(Me$_4$taa) (14, NMR tube scale). To a solution of $[Ti(NNPh_2)Cl_2(py)_2]_2$ (12 mg, 13.1 μmol) in C_6D_6 (0.2 mL) was added a solution of Li_2Me_4taa (4.7 mg, 13.1 μmol) in C_6D_6 (0.2 mL). A color change of the initially cloudy solution to light brown was observed. Analysis by ^{1}H NMR indicated that a reaction had occurred immediately and cleanly to give the known product, Ti(NNPh$_2$)(Me$_4$taa) (**14**).[39]

Ti(NNPh$_2$)(O$_2$NN′)(py) (15). To a stirred solution of $[Ti(NNPh_2)Cl_2(py)_2]_2$ (0.500 g, 1.09 mmol) in toluene (20 mL), cooled to −78 °C, was added a solution of $Na_2O_2NN' \cdot 0.16(THF)$ (0.470 g, 1.09 mmol) in toluene (20 mL) at −78 °C. The solution was allowed to warm to room temperature and then stirred for a further 16 h. The volatiles were removed under reduced pressure to give an oily solid, which was extracted into toluene at −78 °C (2 × 20 mL) and filtered. Volatiles were removed under reduced pressure, and the product was washed with hexane (2 × 10 mL). The brown solid product was dried *in vacuo*. Yield: 0.336 g (49%).

^{1}H NMR (C_6D_6, 299.9 MHz, 293 K): δ 9.21 (2 H, br, 2-C_5H_5N), 9.04 (1 H, d, ^3J = 6.3 Hz, 6-C_5H_4N), 8.31 (4 H, d, ^3J = 8.8 Hz, *o*-C_6H_5), 7.35 (4 H, app. t, app. ^3J = 7.5 and 8.8 Hz, *m*-C_6H_5), 6.94 (2 H, t, ^3J = 7.5 Hz, *p*-C_6H_5), 6.91 (2 H, d, ^4J = 2.1 Hz, 4-$C_6H_2Me_2$), 6.62 (1 H, broad, 4-C_5H_5N), 6.56 (2 H, d, ^4J = 2.1, 6-$C_6H_2Me_2$), 6.38 (1 H, app. t, app. ^3J = 7.9 Hz, 4-C_5H_4N), 6.34 (2 H, br, 3-C_5H_5N), 6.06 (1 H, app. t, app. ^3J = 6.3 Hz, 5-C_5H_4N), 5.70 (1 H, d, ^3J = 7.9 Hz, 3-C_5H_4N), 3.51 (2 H, d, ^2J = 12.5 Hz, $NC\underline{H}_2Ar$ distal to C_5H_4N), 3.20 (2 H, s, $NC\underline{H}_2C_5H_4N$), 2.59 (6 H, s, 3-$C_6H_2\underline{Me}_2$), 2.58 (2 H, d, $NC\underline{H}_2Ar$ proximal to C_5H_4N), 2.25 (6 H, s, 5-$C_6H_2\underline{Me}_2$). $^{13}C\{^1H\}$ NMR (C_6D_6, 75.4 MHz, 293 K): δ 162.9 (2-$C_6H_2Me_2$), 158.1 (2-C_5H_4N), 152.4 (6-C_5H_4N), 151.2(2-C_5H_5N), 147.5 (*i*-C_6H_5), 138.0 (4-C_5H_4N), 132.2 (4-$C_5H_2Me_2$), 129.5 (*m*-C_6H_5), 129.2 (6-$C_5H_2Me_2$), 127.0 (5-$\underline{C}_5H_2Me_2$), 124.5 (3-C_5H_5N), 124.3 (3-$\underline{C}_5H_2Me_2$), 123.2 (1-$C_5H_2Me_2$), 122.0 (*p*-C_6H_5), 121.9 (5-C_5H_4N), 120.8 (3-C_5H_4N), 119.0 (*o*-C_6H_5), 63.4 ($N\underline{C}H_2Ar$), 58.1 ($N\underline{C}H_2C_5H_4N$), 21.1(5 $C_5H_2\underline{Me}_2$), 19.0 (3 $C_5H_2\underline{Me}_2$). IR (NaCl plates, Nujol mull, cm^{-1}): ν 1604 (m), 1595 (s), 1583 (s), 1475 (s), 1444 (s), 1377 (m), 1318 (s), 1272 (s), 1214 (m), 1162 (m), 1102 (w), 1070 (w), 1053 (w), 1039 (m), 1023 (m), 992 (w), 960 (m), 856 (m), 822 (s), 749 (s), 729 (m), 694 (s), 648 (w), 632 (m), 587 (m), 548 (m). EI-MS: *m*/*z* 121 $[OC_6H_2Me_2]^+$ (99%), 105 $[NNPh]^+$ (26%), 91 $[NPh]^+$ (43%), 79 $[NC_5H_5]^+$ (24%). Anal. Found (calcd for $C_{41}H_{41}N_5O_2Ti$): C, 71.9 (72.0); H, 6.0 (6.0); N, 10.2 (10.2).

Crystal Structure Determinations of Ti(NNPh$_2$)Cl$_2$(py)$_3$ (7), Ti(NNPh$_2$)Cl$_2$(py′)$_3$ (8), Ti(NNPh$_2$)(N$_2$N^{C_2,Me})(py) (2), Ti(NNPh$_2$)(N$_2$N^{C_2,SiMe_3})(py) (10), Ti(NNPh$_2$)(N$_2$N^{C_3,Me})(py) (11), and Ti(NNPh$_2$)(N$_2$N^{py})(py) (12). Crystal data collection and processing parameters are given in Table 6. Crystals were mounted on glass fibers using perfluoropolyether oil and cooled rapidly in a stream of cold N_2 using an Oxford Cryosystems Cryostream unit. Diffraction data were measured using an Enraf-Nonius KappaCCD diffractometer. As appropriate, absorption and decay corrections were applied to the data and equivalent reflections merged.[102] The structures were solved by direct methods (SIR92[103]), and further refinements and all other crystallographic calculations were performed using the CRYSTALS program suite.[104] Other details of the structure solution and refinements are given in the Supporting Information (CIF data). A full listing of atomic coordinates, bond lengths and angles, and displacement parameters for all the structures has been deposited at the Cambridge Crystallographic Data Centre. See Notice to Authors, Issue No. 1.

Computational Details. All the calculations have been performed with the Gaussian03 package[105] at the B3PW91 level.[106,107] The titanium atom was represented by the relativistic effective core potential (RECP) from the Stuttgart group (12 valence electrons) and its associated basis set,[108] augmented by an f polarization function (α = 0.869).[109] The remaining atoms (C, H, N) were represented by a 6-31G(d,p) basis set.[110] Full optimizations of geometry without any constraint were performed, followed by analytical computation of the Hessian matrix to confirm the nature of the located extremum as a minimum on the potential energy surface for the experimental complex **2**. For the model systems **Hyd_0**, **Hyd_90**, **Hyd_0_rot**, **Imide_90**, and **Imide_00**, constraints were imposed in the geometry optimiza-

(102) Otwinowski, Z.; Minor, W. *Processing of X-ray Diffraction Data Collected in Oscillation Mode*; Academic Press: New York, 1997.
(103) Altomare, A.; Cascarano, G.; Giacovazzo, G.; Guagliardi, A.; Burla, M. C.; Polidori, G.; Camalli, M. *J. Appl. Crystallogr.* **1994**, *27*, 435.
(104) Betteridge, P. W.; Cooper, J. R.; Cooper, R. I.; Prout, K.; Watkin, D. J. *J. Appl. Crystallogr.* **2003**, *36*, 1487.
(105) Frisch,M. J.; et al. *Gaussian 03, Revision C.02*;Gaussian, Inc.: Wallingford, CT, 2004.
(106) Becke, A. D. *J. Chem. Phys.* **1993**, *98*, 5648.
(107) Perdew, J. P.; Wang, Y. *Phys. Rev. B* **1992**, *45*, 13244.
(108) Andrae, D.; Haussermann, U.; Dolg, M.; Stoll, H.; Preuss, H. *Theor. Chim. Acta* **1990**, *77*, 123.
(109) Ehlers, A. W.; Bohme, M.; Dapprich, S.; Gobbi, A.; Hollwarth, A.; Jonas, V.; Kohler, K. F.; Stegmann, R.; Veldkamp, A.; Frenking, G. *Chem. Phys. Lett.* **1993**, *208*, 111.
(110) Hariharan, P. C.; Pople, J. A. *Theor. Chim. Acta* **1973**, *28*, 213.

tion procedure. For all systems the amido groups NMe_2 and the $N_\beta Me_2$ group (hydrazido models) were constrained to be planar, the pyridine rings were eclipsing the $Ti{=}N_\alpha$ bond. The difference between the various systems lies in the orientation of the amido and/or the hydrazido $N_\beta Me_2$ groups, and these various constraints were imposed upon dihedral angles. In the label of the model systems "0" refers to amido groups lying in the equatorial plane, while "90" refers to amido groups perpendicular to this plane. The label "rot" in **Hyd_0_rot** implies that the $N_\beta Me_2$ group of the hydrazido is perpendicular to the equatorial plane. For all these systems NBO analyses were performed with NBO 5.0 interfaced with Gaussian.[92]

Acknowledgment. We thank the EPSRC for support and Dr. A. R. Cowley for the X-ray structure of **8**.

Supporting Information Available: X-ray crystallographic data in CIF format for the structure determinations of $Ti(NNPh_2)Cl_2(py)_3$ (**7**), $Ti(NNPh_2)Cl_2(py')_3$ (**8**), $Ti(NNPh_2)(N_2N^{C_2,Me})(py)$ (**2**), $Ti(NNPh_2)(N_2N^{C_2,SiMe_3})(py)$ (**10**), $Ti(NNPh_2)(N_2N^{C_3,Me})(py)$ (**11**), $Ti(NNPh_2)(N_2N^{py})(py)$ (**12**), and $Ti_2(\mu\text{-}\eta^2\eta^1\text{-}NNMe_2)_2(O_2NN')_2 \cdot 0.5(C_5H_{12})$ (**16**$\cdot 0.5(C_5H_{12})$). Results and discussion for the attempted synthesis of other titanium hydrazides containing dianionic O_2N_2-donor ligands (**16**, eq S1, Figure S1, Tables S1−S2), comparison between experimental and calculated geometrical parameters for $Ti(NNPh_2)(N_2N^{C_2,Me})(py)$, **2** (Table S3), NPA charges for the model compounds $Ti(NR)(NMe_2)_2(py)_2$ (Table S4), views of selected NLMOs for **Hyd_0** (Figure S2), Cartesian coordinates and electronic energy for the optimized structures, complete list of authors for the reference of Gaussian03. This information is available free of charge via the Internet at http://pubs.acs.org.

OM8007597